Theses and Dissertations | 1. Thesis and Dissertation Collection, all items

1992-12

Evaluations of 404 MHz radar wind profiler observations at Okinawa during TCM-90

Dobos, Paul H.

Monterey, California. Naval Postgraduate School

http://hdl.handle.net/10945/23664

REPORT DOCUMENTATION PAGE		Form Approved OMB No 0704 0188

a REPORT SECURITY CLASSIFICATION	1b RESTRICTIVE MARKINGS
UNCLASSIFIED	

a SECURITY CLASSIFICATION AUTHORITY	3 DISTRIBUTION/AVAILABILITY OF REPORT
	Approved for public release; distribution
b DECLASSIFICATION/DOWNGRADING SCHEDULE	is unlimited.

PERFORMING ORGANIZATION REPORT NUMBER(S)	5 MONITORING ORGANIZATION REPORT NUMBER(S)

a NAME OF PERFORMING ORGANIZATION	6b OFFICE SYMBOL (If applicable)	7a NAME OF MONITORING ORGANIZATION
Naval Postgraduate School	MR	Naval Postgraduate School

ADDRESS (City, State, and ZIP Code)	7b ADDRESS (City, State, and ZIP Code)
Monterey, CA 93943-5000	Monterey, CA 93943-5000

NAME OF FUNDING/SPONSORING ORGANIZATION	8b OFFICE SYMBOL (If applicable)	9 PROCUREMENT INSTRUMENT IDENTIFICATION NUMBER

ADDRESS (City, State, and ZIP Code)	10 SOURCE OF FUNDING NUMBERS			
	PROGRAM ELEMENT NO	PROJECT NO	TASK NO	WORK UNIT ACCESSION NO

TITLE (Include Security Classification)
Evaluations of 404 MHz Radar Wind Profiler Observations at Okinawa During TCM-90

PERSONAL AUTHOR(S)
Dobos, Paul H.

a TYPE OF REPORT	13b TIME COVERED		14 DATE OF REPORT (Year, Month, Day)	15 PAGE COUNT
Master's Thesis	FROM _____ TO _____		1992, December	92

SUPPLEMENTARY NOTATION
The views expressed in this thesis are those of the author and do not reflect th
official policy or position of the Department of Defense or the U.S. Government.

COSATI CODES			18 SUBJECT TERMS (Continue on reverse if necessary and identify by block number)
FIELD	GROUP	SUB-GROUP	Okinawa, radar wind profiler, rawinsonde, regression,
			statistics, TCM-90, tropical cyclone, typhoon,
			wind prediction, wind ratios

ABSTRACT (Continue on reverse if necessary and identify by block number)

A comparison is made of rawinsonde and radar wind profiler observations recorded in Okinawa during the Tropical Cyclone Motion (TCM-90) field experiment. The rawinsondes were launched from Naha, 18.5 km south-southwest of the wind profiler at Kadena AB. An examination of wind speed, and u- and v-components shows the two wind measuring systems to be in excellent agreement. Wind speed differences are less than 1.5 m/s, and u- and v-component differences are less than 2 m/s.

Surface wind data recorded 1.5 km from the radar wind profiler site at Kadena are used to derive statistical relationships between the wind at the five lowest profiler range gates and the surface sustained wind and gusts. The accuracy of regression equations derived from the surface and upper-level data is compared to that of simple wind ratios derived from the same data. The data are also stratified with respect to daytime versus nighttime, and winds having a trajectory from the ocean versus winds with a trajectory from the land. Although the regression equations generally produce a

DISTRIBUTION/AVAILABILITY OF ABSTRACT	21 ABSTRACT SECURITY CLASSIFICATION
☐ UNCLASSIFIED/UNLIMITED ☐ SAME AS RPT ☐ DTIC USERS	UNCLASSIFIED

NAME OF RESPONSIBLE INDIVIDUAL	22b TELEPHONE (Include Area Code)	22c OFFICE SYMBOL
R.L. Elsberry	408-656-2373	MR/Es

Form 1473, JUN 86   Previous editions are obsolete   SE
S/N 0102 LF 014 660

T260099

Block number 19 Continued:

statistically significant smaller prediction error compared to prediction errors from the ratios, the less than 2 m/s improvement in surface wind estimates is not operationally significant.

Evaluations of 404 MHz Radar Wind Profiler Observations
at Okinawa During TCM-90

by

Paul H. Dobos
B.S., Pennsylvania State University, 1987

Submitted in partial fulfillment of the
requirements for the degree of

MASTER OF SCIENCE IN METEOROLOGY

from the

NAVAL POSTGRADUATE SCHOOL
December 1992

ABSTRACT

A comparison is made of rawinsonde and radar wind profiler observations recorded in Okinawa during the Tropical Cyclone Motion (TCM-90) field experiment. The rawinsondes were launched from Naha, 18.5 km south-southwest of the wind profiler at Kadena AB. An examination of wind speed, and u- and v-components shows the two wind measuring systems to be in excellent agreement. Wind speed differences are less than 1.5 m/s, and u- and v-component differences are less than 2 m/s.

Surface wind data recorded 1.5 km from the radar wind profiler site at Kadena are used to derive statistical relationships between the wind at the five lowest profiler range gates and the surface sustained wind and gusts. The accuracy of regression equations derived from the surface and upper-level data is compared to that of simple wind ratios derived from the same data. The data are also stratified with respect to daytime versus nighttime, and winds having a trajectory from the ocean versus winds with a trajectory from the land. Although the regression equations generally produce a statistically significant smaller prediction error compared to prediction errors from the ratios, the less than 2 m/s improvement in surface wind estimates is not operationally significant.

TABLE OF CONTENTS

LIST OF TABLES

LIST OF FIGURES

ACKNOWLEDGEMENTS

I. INTRODUCTION

The Naval Postgraduate School (NPS) 404 MHz Doppler wind profiler was operated at Kadena ab on Okinawa in support of the Tropical Cyclone Motion 1990 (TCM-90) field experiment from 16 August to 28 September 1990 (Elsberry *et al.* 1990). In this six week period of wind measurements (Fig. 1), three typhoons passed within 250 km of the profiler site: Typhoon (TY) Abe, 250 km to the south; Supertyphoon (STY) Flo, 110 km to the east; and TY Gene, 185 km to the southwest. The site was on the fringes of three more distant typhoons: Yancy, Dot and Zola. Wind speeds measured by the wind profiler ranged from near calm to over 40 m/s in ST Flo.

This radar wind profiler data study has two parts. Section II is a comparison between rawinsonde and profiler data. Here the profiler data set is contrasted with rawinsonde data from Naha, which is located 18.5 km south-southwest of Kadena. This is one of the first comparisons in the tropical environment under such a large range of wind conditions and with a 404 MHz wind profiler. Section III is an investigation of the boundary layer structure over a large range of wind speeds at a fixed site. Regression equations for the surface wind are derived from upper-level (wind profiler) and surface wind observations at Kadena ab.

A.   RADAR SPECIFICATIONS

An overview of the theory behind microwave radar wind profilers is presented by van de Kamp (1988), while Ottersten (1969) provides a more general, physical investigation of clear-air radar. Some basic principles involved in radar wind profiling are described here.

1
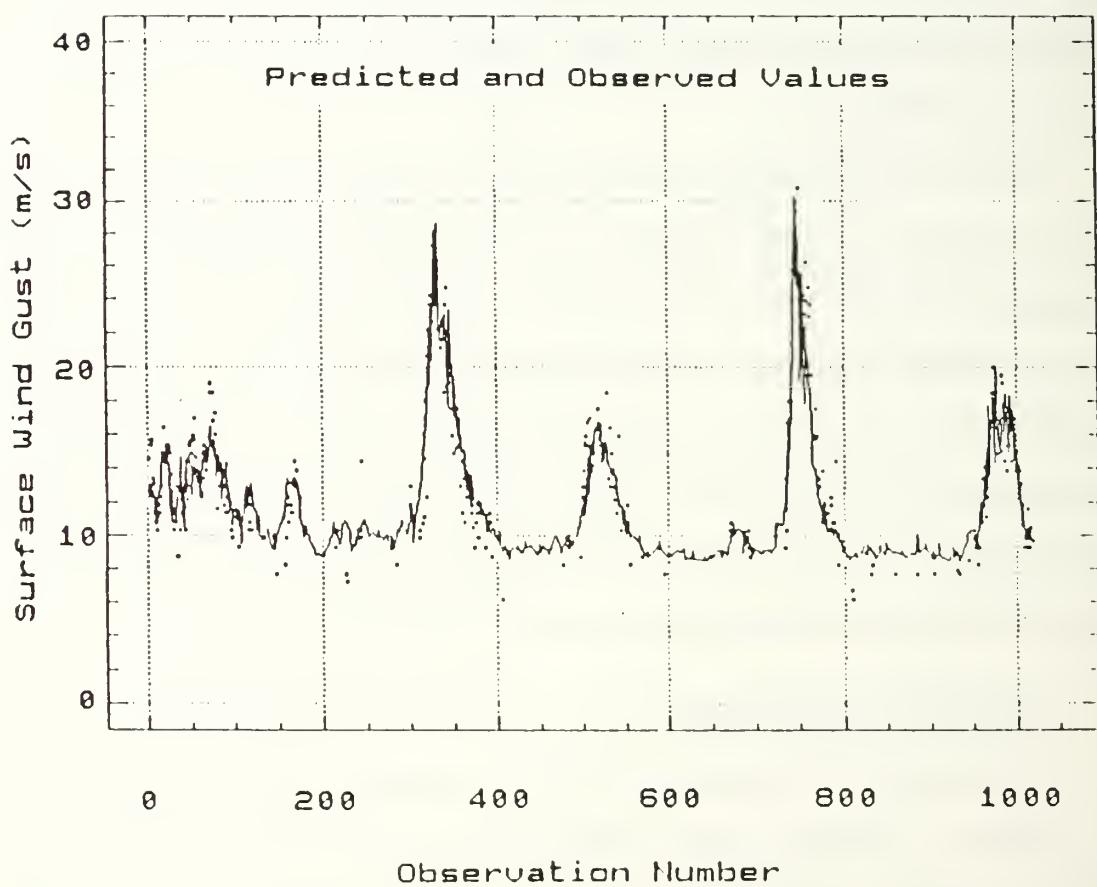
Fig. 1. Observed (dots) and fitted (solid) values of surface wind gusts at Kadena AB, Okinawa during TCM-90. The four prominent peaks at approximately observation number 350, 525, 750 and 975 are due to the proximity of TY Abe, TY Dot, STY Flo and TY Gene, respectively.

2

Standard wind profilers are pulsed emission (rather than continuous wave) Doppler radars that emit electro-magnetic energy in the 50 to 1280 MHz range. They typically use phased arrays of coaxial-collinear antenna elements to point the radar in two to five directions. The NPS radar has three "beams": one vertical and two that are tilted 15° from the vertical while also being perpendicular to each other.

After a pulse has been emitted in a particular direction, the radar antenna becomes a receiver and records the reflected radiation, which will be referred to as an "echo." A number of echoes received from a given direction (along the beam) are averaged, which is called time-domain averaging. A set of 256 time-domain averages are then converted to a frequency spectrum of Doppler shifts. The difference between the emitted and echo frequencies (the Doppler shift) determines the radial wind velocity along a particular beam. The time delay from the transmitted pulse to the echo receipt determines the height of the wind measurement. Successively larger time delays then establish "range gates" at higher elevations.

The reflectivity of an object in the atmosphere is dependent upon the wavelength of a radar. Wind profilers rely on Bragg scattering, so that objects with a length scale that is one half the wavelength of the radar will best reflect (backscatter) radio frequency radiation. The frequency of the NPS radar is 404 MHz, which corresponds to a 0.74 m wavelength. Therefore, the best backscatterers are objects that have a scattering cross-section of 0.37 m. In the atmosphere, objects of this dimension are turbulent eddies formed by gradients of velocity, temperature and moisture. In addition to echoes by objects that are about a third of a meter, a fraction of the emission will be backscattered from objects both

3

larger and smaller than this ideal size, especially those objects that are more highly reflective than the optimum size eddies. Thus, erroneous winds are possible from Doppler shift spectra that have been contaminated by reflections from rain, aircraft or other non-representative scatterers that are not moving with the wind. In addition, strong returns are possible when large numbers of objects much smaller than the ideal size (e.g., rain), form a highly reflective scattering cross-section. Section B below will address this problem.

The typical operation of the NPS wind profiler utilizes pulse lengths of 250 m and 1000 m. The 250 m pulse allows for independent measurements of wind with a fine vertical resolution (250 m for each range gate) up to an average elevation of about 9000 m (higher elevations are observed in a more turbulent atmosphere). Above this height, backscatter radiation from this pulse length generally can not be distinguished from noise in the radar system. Due to the narrow, more focused beam, the 1000 m pulse generally can retrieve data from greater heights (16 km winds were recorded in a typhoon environment). For measurements to be independent, the resolution must decrease to 1000 m. Otherwise, a single pulse would overlap several range gates.

Measurements are made in 36 range gates for both the short and long pulse lengths. At Kadena, the first measurement (lowest gate) was set at 600 m for the 250 m pulse, and the remaining 35 range gates were spaced every 300 m. Thus, the wind measured in these gates was independent of the wind measured at the gates above and below. The 1 km pulses started at 6 km and used a 375 m gate increment. As a consequence, the wind profile from the 1 km pulse has been "smoothed" because of the pulse overlapping gates.

4

A 256 point Fast Fourier Transform (FFT) is used to convert the time series of echo power at an individual gate to a power spectrum of Doppler shifts. From this spectrum, many quantities are calculated for each beam: the spectral width, noise and most importantly, the signal power of the spectral peak. The radial velocity is found from the Doppler shift frequency that is identified by the spectral peak. Knowing the direction that each beam points and the radial velocity for each beam, the three components of the wind (u, v and w) are calculated from geometrical relationships. The wind direction and speed are calculated from u, v and w for each range gate (elevations above the radar) to give a wind profile directly over the site.

B.   CONSENSUS ALGORITHM

For all three beams and for each range gate, the Doppler radar wind profiler creates a complete set of measurements approximately every six minutes. Therefore, up to 10 sets of winds per gate are available each hour. The purpose of the consensus algorithm is to eliminate questionable winds and calculate a representative wind for that hour from the "six-minute winds." The consensus algorithm used here is described in detail by Lind (1993), who enhanced the algorithm provided by the manufacturer. A brief overview is presented by Dobos *et al.* (1991). The modification was necessary because the manufacturer's consensus algorithm was unable to accurately handle cases with heavy convective rainfall (typical of tropical precipitation).

Lind's consensus algorithm has seven steps:
1. Signal/Noise Ratio Check of Six-minute Data
2. First-guess Consensus Profile
3. Wind Shear Check

4. Cubic Spline Interpolation to Fill-in Missing Levels

5. Best Fit Profile

6. Wind Shear Check

7. Final Wind Profile

The signal-to-noise ratio check (step 1) eliminates those radial velocities that were computed from weak echos (signal strength less than -20.5 dB). The second step is the formation of a first-guess (Raw Target in Fig. 2) by an elaborate scheme that calculates consensus winds for each range gate from the six-minute radial velocities received each hour. The algorithm calculates consensus winds from all observations that have radial velocities (DV_r) within 6.5, 6.0, 5.5, 5.0, ... 2.0, 1.5 and 1.0 m/s of each other (12 in total). From these 12 consensus winds, the first-guess consensus wind profile is made (step 2). The first-guess profile is dependent on altitude and pulse length. For the 250 m pulse (1000 m pulse) and range gates below 7 km (9 km), consensus winds that have radial velocities within 6 m/s of each other ($DV_r=6$) are used. For altitudes between 7 km (9 km) and 8 km (10 km), the first-guess wind is derived from radial velocities corresponding to $DV_r=5$. For altitudes between 8 km (10 km) and 9 km (11 km), the profile includes winds with radial velocities of $DV_r=4$. Winds derived from radial velocities that are within 3 m/s from each other ($DV_r=3$) are used for range gates between 9 km (10 km) and 10 km (12 km). Those gates at 10 km (12 km) and above use winds with $DV_r=2$. This initial profile of consensus winds is the starting point for the consensus algorithm.

The vertical wind shear check (step 3) eliminates observations that have a strong signal-to-noise ratio (e.g., rain-contaminated winds) but are grossly different from the wind observations above or below. This rudimentary check is dependent
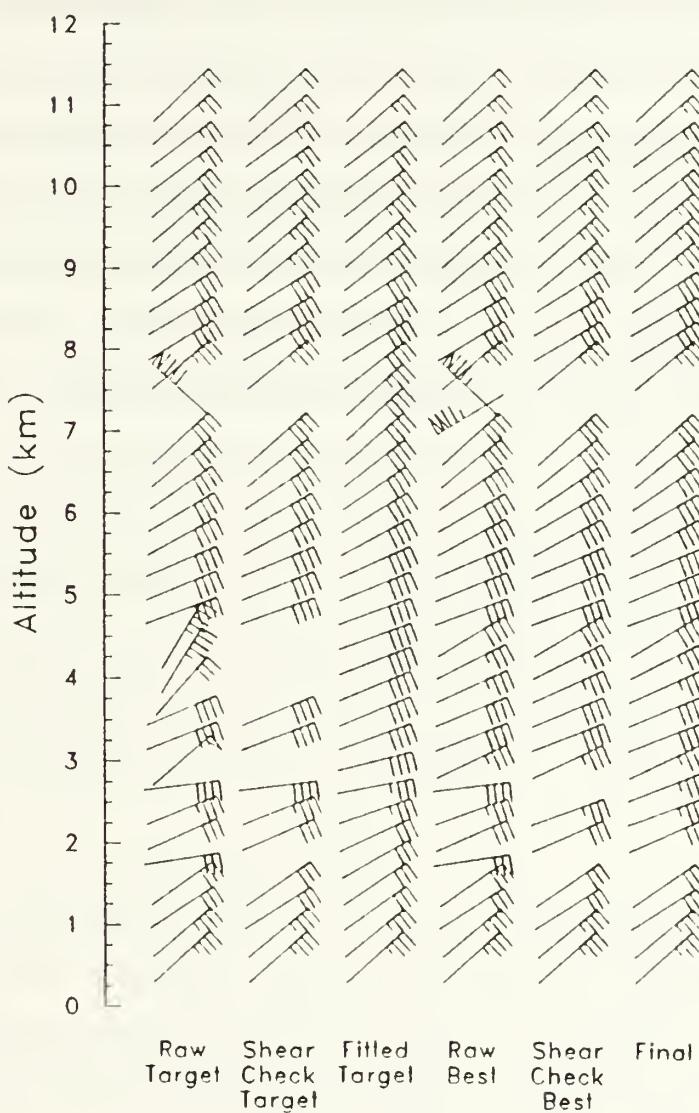
Fig. 2. Wind observations (full barb = 5 m/s) from six of the seven steps in the Lind (1993) consensus algorithm (see text).

on the wind speed. The observation is not used if the wind speed is below 20 m/s and the shear is more than 10 m/s in one kilometer. If the wind speed is greater than 20 m/s, the observation is removed when shear in one kilometer is more than one half the wind speed.

The goal of steps 4-6 is to find a vertical profile of winds that is complete (with a minimum of missing data) and reasonable (having no gross shears). Gaps in the initial shear checked "target" profile are replaced by an interpolated value. This is accomplished by calculating cubic spline coefficients for the valid u- and v-component profiles of the shear-checked winds from step 3. The missing data in each profile are then "filled-in" with winds comprised of u- and v-components calculated from the spline coefficients (Fitted Target in Fig. 2). This "filled-in" profile is then used as a "target" to find a real wind in the next step.

The fifth step selects the wind (from the 12 DV_r's) that has the smallest root-mean-square (RMS) difference when compared to the Fitted Target wind for that level. It should be understood that this wind is a real wind (Raw Best in Fig. 2) and not an interpolation. That is, actual observed winds have been selected to fill-in the data removed by the vertical shear check. By selecting the wind that is the most similar to the target wind, it is highly probable that the consensus profile is reasonable.

The sixth step, as in step 3 above, is a vertical shear check that discards any wind that grossly differs from the wind in an adjacent range gate. This is primarily a check to see if the winds chosen to fill-in the missing winds are reasonable. In the seventh step, an attempt is made to replace observations that were removed by the step 6 shear check with another DV_r, and particularly, one that comes close to the Raw Best (Fig. 2) and does not violate the shear check.

8

The above sequence of steps is different from other consensus algorithms. For example, when determining the horizontal wind, the original algorithm will indicate missing data if three out of six radial velocities are not within 2 m/s ($DV_r=2$) of each other. By contrast, the Lind (1993) algorithm will accept as few as a single radial velocity if it passes a number of quality control checks. As another example, once the original consensus algorithm picks a consensus wind based on $DVr=2$, it does not do a quality control on the selected wind. Lind (1993) included steps 3-7 above for this purpose and for finding an alternative, but reasonable wind if the first selection does not pass a shear check. The advantage of the Lind (1993) algorithm becomes apparent in a combined rain and high wind condition. While the original algorithm may generate erroneous winds, the Lind algorithm includes quality control steps to identify such winds and attempts to find valid replacements.

II. RAWINSONDE AND PROFILER COMPARISON

A.   BACKGROUND AND OBJECTIVE

Nearly 50 years have passed since rawinsondes were first used to measure the winds aloft. Since that time, a network of about 1000 upper-air stations has evolved worldwide. As most of these observation sites are located in the most populous regions of the globe, i.e., continental Northern Hemisphere, rawinsonde wind measurements generally are not available over the vast majority of the earth's surface that is oceanic. Rawinsonde observations (raobs) are not affordable for many non-industrial nations. Raobs are expensive, require trained personnel and both permanent and non-recoverable equipment.

Wind observations are important inputs to weather prediction models. This is especially true for tropical regions, where the mass field adjusts to the wind field during the model initialization. Unfortunately, a paucity of rawinsonde sites exists in the tropics, where wind data are most needed. A possible solution to this dilemma is the radar wind profiler, which is wind-sensing equipment with a high initial cost, but a low operating cost. The 404 MHz profiler that operated at Okinawa automatically provided horizontal and vertical wind data from 300 m to typically 10 km (above 16 km in a storm environment) every six minutes. The observations were then converted to hourly wind profiles by the consensus algorithm described in Section I.

Thomson and Williams (1991) compared various types of wind-measuring instruments, including Doppler radar wind profilers and rawinsonde equipment. A linear regression of the winds recorded by two receivers tracking the same rawinsonde had a standard deviation of 1.41 m/s between the data and the fitted line. Similarly, a regression of the winds at 1500 m from two collocated wind

10

profilers had a standard deviation between the data and the fitted line of 0.91 m/s. Based on this smaller standard deviation, Thomson and Williams (1991) recommended that Doppler-based systems (vice rawinsondes) should be the standard wind-measuring instruments.

May (1992) of the Australian Bureau of Meteorology Research Centre compared 50 MHz radar wind profiler winds with 120 rawinsonde soundings collocated at Saipan during TCM-90 (Elsberry *et al.* 1990). Below 10 km, the root-mean-square (RMS) differences between the rawinsonde and profiler u-components and v-components were 2.5 m/s and 2.1 m/s respectively. Between 10 and 18 km these RMS differences increased about 75% to values of 4.4 m/s and 3.7 m/s respectively. The May (1992) study is the first intercomparison of data from rawinsondes collocated with a radar wind profiler in the tropics. It is encouraging that May (1992) found smaller wind speed differences than any prior rawinsonde-profiler comparison.

In this Section, rawinsonde observations from Naha, Okinawa are contrasted with the 404 MHz radar wind profiler observations at Kadena ab, Okinawa (18.5 km separation distance).

B. METHOD

The comparison of rawinsonde data and wind profiler data is not a straight-forward process. A direct comparison between the wind at a particular profiler level (center of a range gate) and the rawinsonde observation requires an interpolation between the mandatory and significant levels in the Naha raobs since the raw (one or two minute data) are not available. This interpolation process is made more complicated because the raobs do not include the heights (only the pressures) of the

significant wind levels. Furthermore, the depth over which the raob winds are to be averaged, need to be made comparable with the radar pulse length.

The heights of the significant wind levels are approximated with a logarithmic pressure interpolation

$$Z = Z_b \frac{- \ln (P_b / P) * (Z_b - Z_a)}{\ln (P_b / P_a)} \quad ,$$

where P is pressure, Z is the height of the pressure surface, and the subscripts b and a indicate levels below and above. That is, the nearest heights above and below the level with the missing height are used along with the natural log of the pressures to interpolate the missing height.

The wind profiler pulse length (250 m or 1000 m) for a particular range gate is used to determine the appropriate averaging layer of the rawinsonde winds for comparison with profiler winds. For example, rawinsonde winds from 1500 m plus and minus 125 m (1/2 of pulse length) are averaged to compare with the profiler winds at 1500 m where the pulse length is 250 m (Fig. 3).

Each rawinsonde direction and speed report is decomposed into u- and v-components and separate cubic splines are fit for each component with elevation. From these splines, wind components can be easily and accurately interpolated for any altitude within the interval used to determine the spline coefficients. For the 1500 m gate comparison (Fig. 3), u- and v-components from the raob are calculated from the spline coefficients in 25 m increments (100 m increments for 1000 m pulse lengths) for the layer from 1375 to 1625 m. These 11 u-components are averaged
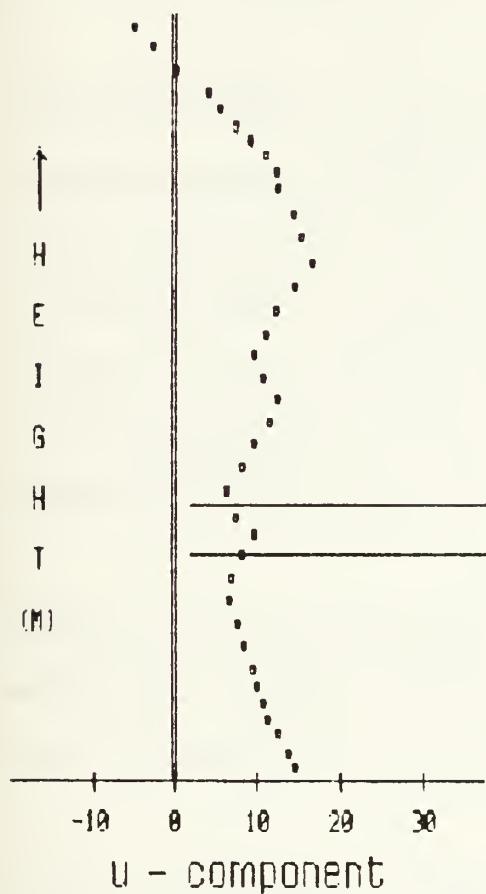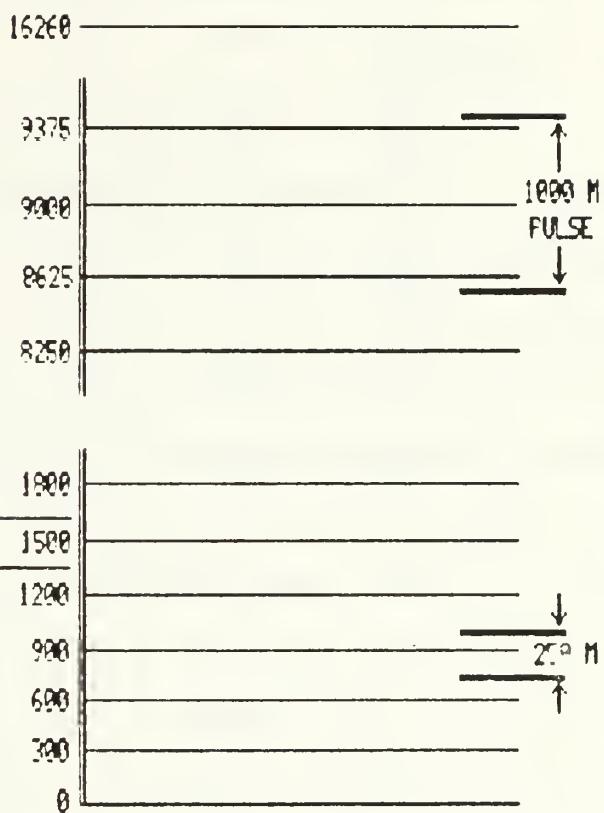
Fig. 3. Schematic representation of the spatial relationships between rawinsonde (left) and radar wind profiler (right) data (see text).

13

and combined with the average of the 11 v-components to define the rawinsonde wind direction and speed that correspond to the wind at the profiler gate.

The data set contains 94 rawinsonde observations separated by 6 h during intensive observing periods and 12 h at other times (Elsberry *et al.* 1990). Each wind profiler sounding contains winds from about 36 gates. These are matched with the rawinsonde winds to yield 3520 comparisons.

C.   RESULTS

The magnitudes of the differences between the rawinsonde and profiler winds are computed separately for wind speed, and for the u- and v-components. Means and medians of the 3520 wind differences as well as standard deviations are recorded in Table 1. The u- and v-component differences are about 2 m/s (with 2.7 and 2.0 m/s standard deviations). These results are smaller than the component differences obtained by May (1992) by 0.6 and 0.2 m/s for the u- and v-components below 10 km, and 2.5 and 1.8 m/s above 10 km. The mean wind speed difference is about 1.5 m/s with a standard deviation of 1.4 m/s.

Biases for the wind speed and u and v component differences are all less than 0.5 m/s, and thus are insignificant. The correlation coefficients between the rawinsonde and profiler wind speeds and components are impressive (96% and better).

The rawinsonde and profiler wind differences summarized above are expected to be a function of wind speed and altitude (i.e., the differences should increase if the wind speed or height increases). Thus, the direction and speed differences are stratified with respect to rawinsonde wind speed and height in the following subsections.

Table 1.   DIFFERENCES, BIASES AND CORRELATION COEFFICIENTS BETWEEN RADAR WIND PROFILER AND RAWINSONDE MEASUREMENTS.   Sample size is 3520 pairs of observations.   Difference is defined as the absolute value of the difference between the two measurements. Bias is the rawinsonde value minus the profiler value. $\bar{X}$ is the sample mean and S is the standard deviation.

STATISTICS		SPEED (m/s)	U (m/s)	V (m/s)
Difference	$\bar{X}$	1.5	1.91	1.92
	S	1.4	2.71	1.95
	Median	1.1	1.21	1.36
Bias (R-P)	$\bar{X}$	0.1	0.20	-0.49
	S	2.0	3.31	2.69
	Median	0.2	-0.21	-0.40
Correlation Coefficient		0.97	0.96	0.97

15

1.   Wind Speed Differences Versus Rawinsonde Speed

The overall sample of the profiler wind speeds versus the rawinsonde wind speeds (Fig. 4a) has a concentration of speed observations below 20 m/s. At higher speeds, more scatter around the mean is found. The accuracy of the rawinsonde should be greater in higher wind speeds because the horizontal displacements being detected by the Omega navigation system will be larger. However, the profiler and rawinsonde winds have a greater probability of being different during high wind speeds because a rawinsonde balloon is more likely to have been carried farther from the wind profiler site than in light wind situations.

The entire set of wind differences is divided into four ranges of rawinsonde wind speeds with equal numbers of observations (Fig. 4b). Each box plot represents the distribution of rawinsonde and profiler speed differences when the rawinsonde speed is in one of four ranges: less than 7.9 m/s, greater than or equal to 7.9 m/s but less than 12.5 m/s, between 12.5 m/s and 19.2 m/s, and greater than 19.2 m/s. When the raob speed is less than 7.9 m/s, for example, the median is approximately zero with one half of the speed differences between 1 and -1 m/s. The only statistically significant differences in medians among the four subsets are for the two highest wind speed ranges, since the notches that represent the 95% confidence intervals do not overlap in these two subsets. However, such a small difference between the medians (less than 0.5 m/s) is not meteorologically significant. Thus, the median difference between the rawinsonde speed and the profiler wind speed does not vary as a function of the wind speed in this sample.

The increased scatter that was observed in the scatter plot (Fig. 4a) for the higher rawinsonde speeds is also indicated in the two box plots with winds greater than 12.5 m/s. Therefore, even though the median rawinsonde/profiler
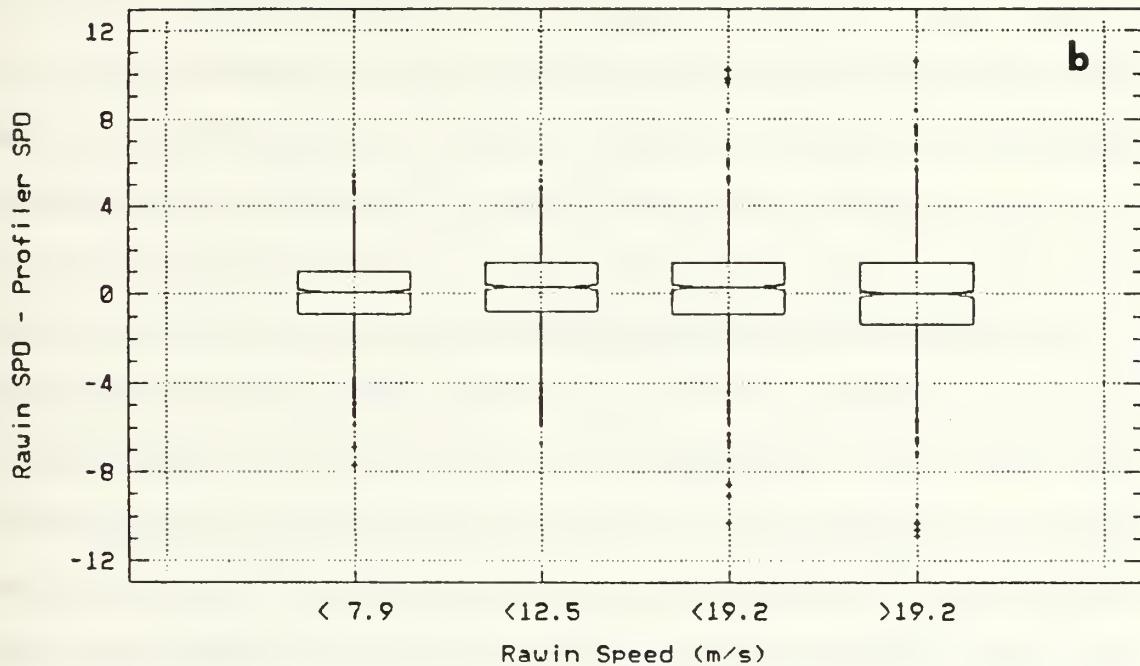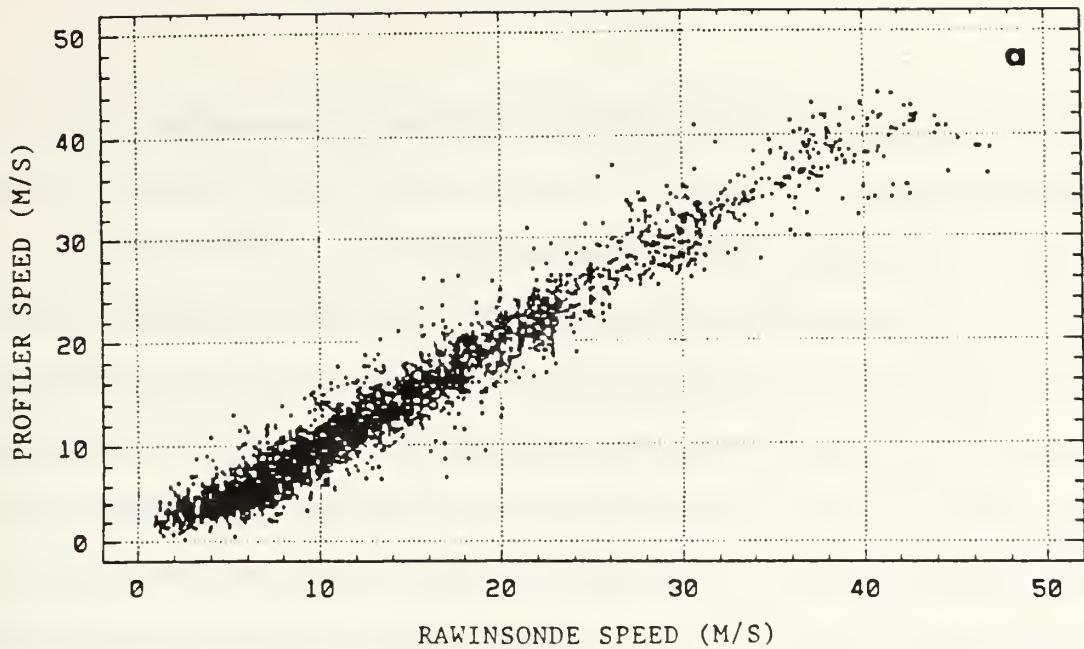
Fig. 4. (a) Scatterplot of rawinsonde versus wind profiler wind speeds (m/s). (b) Box plots of rawinsonde and wind profiler wind speed differences as a function of rawinsonde speed (m/s). The horizontal line through the box gives the value of the median of the distribution, while the box dimension gives the range in which 50% of the data falls. The notches on the box give the 95% confidence interval for the median. The range of values between the top and bottom of the box is defined as the "interquartile range." A vertical line extends to the largest value that is within 1.5 times the interquartile range above the top of the box, and the smallest value within 1.5 times the interquartile range below the bottom. Additional symbols above and below the vertical lines show actual data values (outliers).

17

wind speed difference does not change as the wind speed increases, the variance (or scatter) does increase.

2.   Wind Speed Differences Versus Height

Only in the absence of horizontal wind would the rawinsonde balloon be expected to have an ascent directly above the site, which is the column of air measured by the profiler. Because of the downstream balloon drift with increasing elevation in most cases, the differences between the raob wind speed and the profiler wind speed would be expected to increase as a function of height. In addition, the radar wind profiler observations are expected to be less accurate at the uppermost range gates as the returned signals decrease in magnitude and finally become indistinguishable from the noise in the system. To describe this elevation dependence, the distribution of speed differences is separated into four equal subsets based on height above ground: below 3315 m, between 3315 and 6010 m, between 6011 and 7885 m, and heights greater than 7886 m. A concentration of data occurs in the layer between 6011 and 7885 m because it is here that profiler wind data are received from both the 250 and 1000 m pulses. A trend toward larger median differences in rawinsonde/profiler wind speeds with increased balloon height is evident in Fig. 5a. However, the 95% confidence intervals (indicated by the notches in the boxes) show the median speed differences of adjacent layers are not significantly different. The wind differences in the 6011 to 7885 m layer have the smallest range of values. Wind observations above this layer typically would have more balloon drift so that these differences are associated with the greater spatial separations from the profiler site. Some other explanation is required for why the wind speed difference variances are higher at altitudes below 6011 m.

A three-dimensional display of rawinsonde/profiler wind speed versus height (Fig. 5b) illustrates the larger scatter at low altitudes when the wind speeds are high (greater than 25 m/s). This larger scatter may be explained by the uneven terrain of Okinawa and the 18.5 km separation distance between the profiler and the rawinsonde launch site. As the low-level flow over the rough terrain increases, the flow becomes more turbulent, which decreases the correlation between the two wind measurements. Although this boundary layer explanation would apply primarily in the layer below 3315 m, the convection in the passing typhoons that generated these larger wind speeds would also extend into the 3315-6010 m layer.

3.   U- and V-Components

Interpretations of the u- and v-components as a function of speed and height provide similar information as in the discussion above. For completeness, these box-plots and 3-D scatter plots are included in the Appendix A.

4.   Summary

The correlation between rawinsonde and profiler wind speeds and components is very high (96% and better), which gives a difference of 1.5 m/s for the wind speed and 2.0 m/s for the u- and v-components. Three-quarters of the wind speed data are below 20 m/s and have a median difference (between the rawinsonde and profiler data) that does not change as the wind speed changes. Over one half of all of the wind speed differences fall between $\pm$ 1.5 m/s. Larger variance is noted when the wind speed is above 12.5 m/s. Wind speed differences below 3315 m have larger variance (compared to other heights) when the wind speed is greater than 25 m/s. The best wind speed correlation occurs in the 6011 - 7886 m layer.
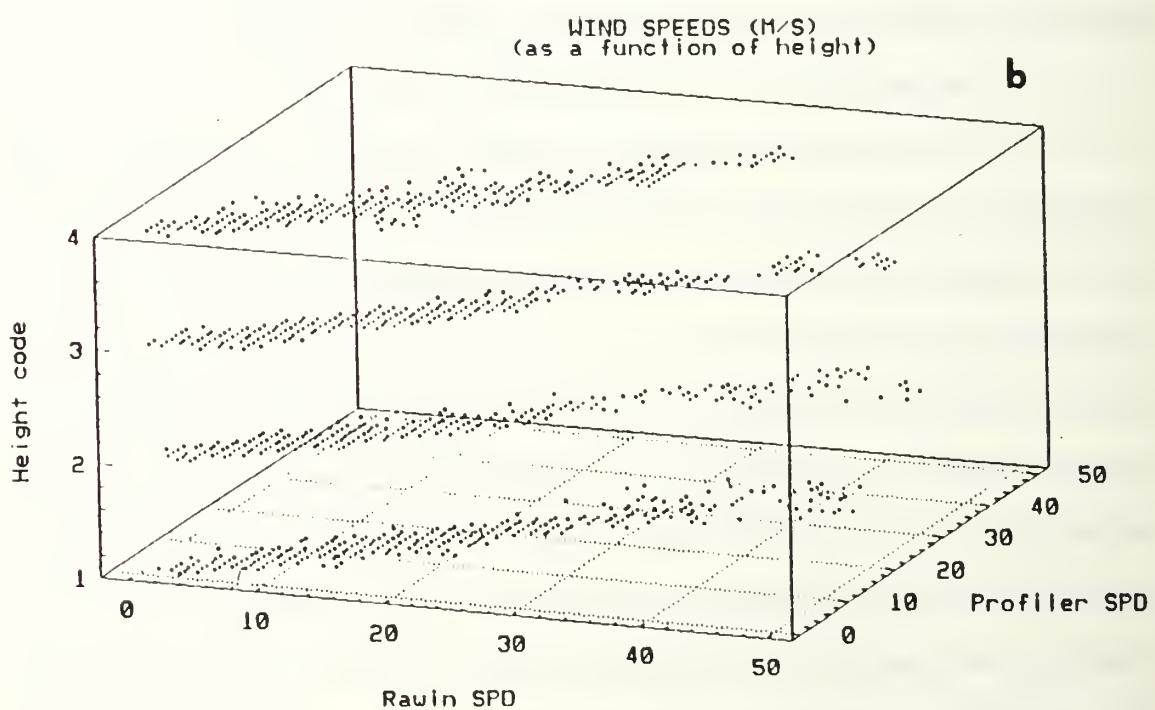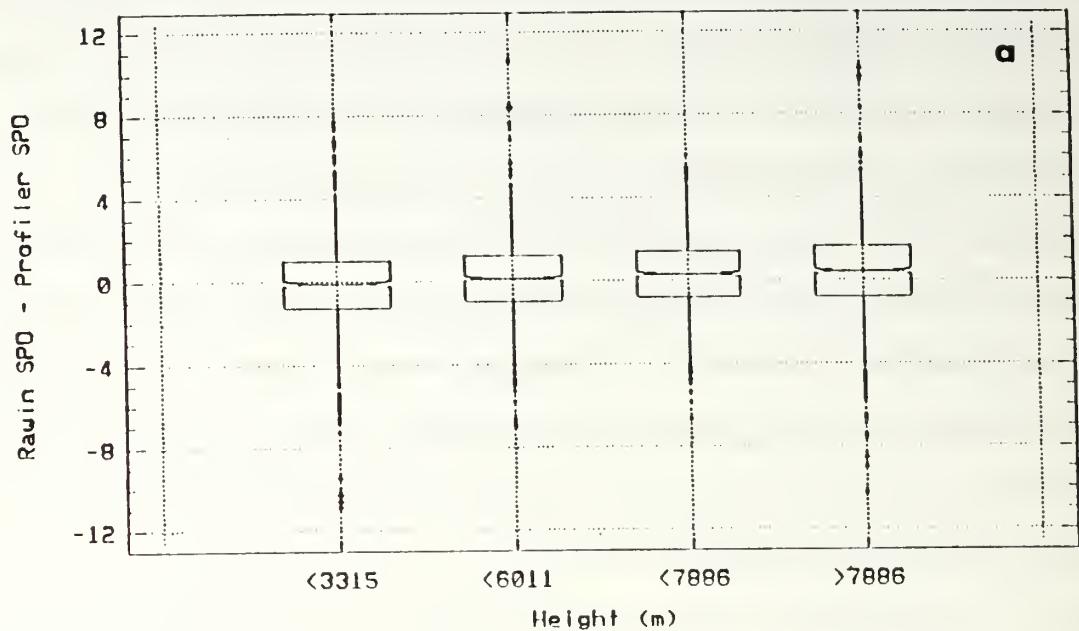
Fig. 5. (a) Box plots of rawinsonde and wind profiler wind speed differences as in Fig. 4b, except as a function of height. (b) 3-D scatterplot of rawinsonde wind speed versus wind profiler wind speed (m/s) for the four height intervals.

III. BOUNDARY LAYER WIND ANALYSIS

Wind observation platforms such as aircraft and satellites only transmit or sense winds aloft. It would be advantageous to weather forecasters (especially those responsible for the data-sparse tropics) if the upper-level winds available from these sensors could be related to the surface wind (speed, gust and direction). In this way, estimated surface wind conditions would be available for forecasts, warnings and disaster preparedness decisions. Alternately, the derived relationships between the upper-level and surface winds can also be used to estimate the wind aloft when only the surface wind observations are available.

A. BACKGROUND AND OBJECTIVE

Using aircraft data collected in three hurricanes as the input, Powell (1980) compared wind predictions from four marine boundary-layer models to 20 observed winds from buoys and ships. Three of the models, as well as an empirical 0.8 ratio, related the near-surface wind speed to the upper-level observations to within 10% accuracy. Powell (1982) adjusted wind data from aircraft, ships, buoys and land stations to a 10 m height and then composited them relative to the center of Hurricane Frederic for both open water and landfall positions. Over open water, a 0.7 ratio best related upper-level (500 - 1500 m) observations to the 10 m winds, while a 0.56 ratio was determined best for land-based, near-surface wind predictions. In addition, Powell concluded that 0.8 times the upper-level wind is the best predictor of the surface gust over the land.

Powell *et al.* (1991) investigated the vertical and horizontal wind structure in Hurricane Hugo, and computed ratios to predict surface sustained winds and gusts from aircraft reconnaissance winds. Table 2 (from Powell *et al.* 1991) is a summary

TABLE 2. MEAN RATIOS OF SURFACE MEAN WIND AND GUST TO FLIGHT-LEVEL MEAN AND MEAN SURFACE GUST FACTORS FROM COMPARISONS OF SURFACE AND AIRCRAFT DATA IN LANDFALLING HURRICANES (Powell *et al.* 1991).

Storm	Number of Observations	Sustained Wind Ratio	St.Dev.	Gust Ratio	St.Dev.
Frederic '79	18	0.58	0.10	0.88	0.11
Alicia '83	13	0.59	0.14	0.95	0.21
Hugo '89	18	0.49	0.13	0.73	0.18

of empirically derived wind ratios for three hurricanes. The ratio of the surface wind over land to the wind aloft ranges from 0.49 to 0.59, while the ratio of land gusts to winds aloft varies from 0.73 to 0.95. Although these findings are useful, it should be noted that many of the surface wind speeds used in Powell (1982) and Powell *et al.* (1991) were estimated from different heights above ground, and had large space and time separations from the upper-level data. Thus, it would be useful to derive wind relationships from measured (rather than estimated) winds and use as small a space and time separation as possible when linking the upper- and lower-level winds. These requirements were fulfilled in this study by using a TCM-90 data set (Elsberry *et al.* 1990) that contained radar wind profiler winds and surface winds from Okinawa, Japan.

B.   METHOD

Data obtained from a 404.37 MHz wind profiler at Kadena ab in Okinawa are used to derive relationships between the surface winds and those aloft. Unlike studies that use composite data from different times and locations, all of the observations in this dataset are from the same site and at exactly the same elevation above the ground. A set of 1022 hourly wind observations from the 600, 900, 1200, 1500 and 1800 m range gates are related to the surface winds through a multiple (stepwise) least-square regression. One goal is to derive the empirical relationships that can be applied to upper-level winds obtained by aircraft or satellites to predict the surface condition. Conversely, given a surface wind observation from a land station, an estimate could be made of the wind above the station in a tropical cyclone.

The radar wind profiler site was less than 0.5 km from the shore on the southwest side of Okinawa (Fig. 6). The surface wind observation site was located

approximately 1.5 km inland from the radar location and approximately 38 m higher

than the radar ground plane. Surface sustained wind and gust observations were
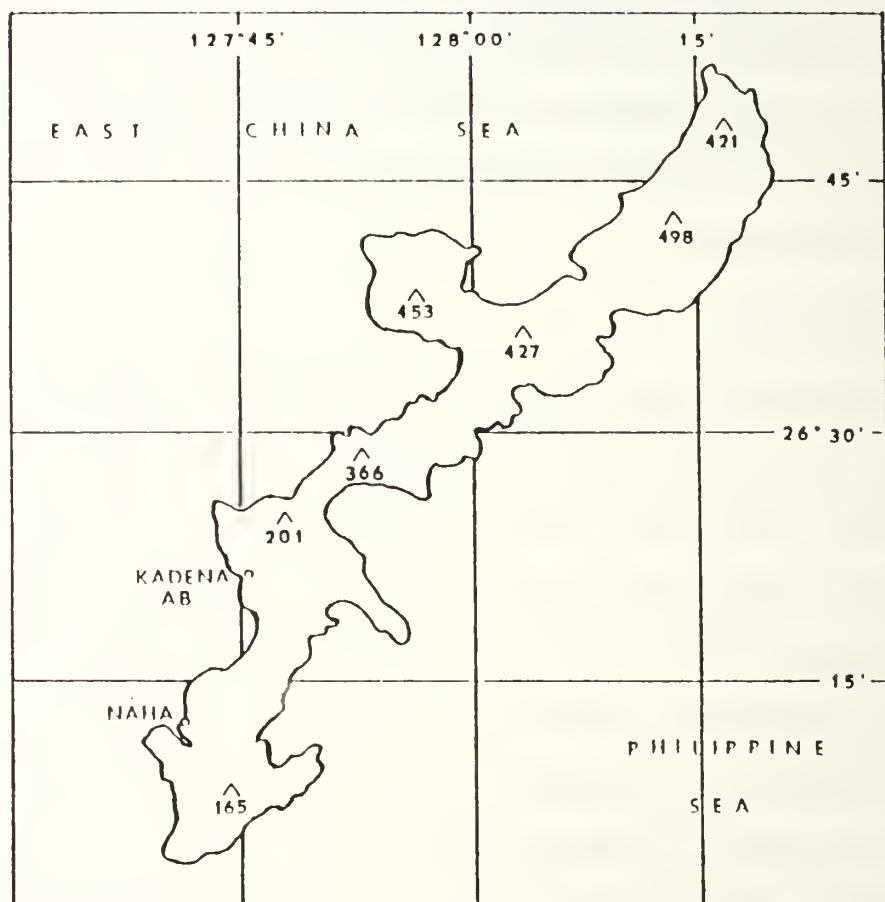
Fig. 6. Map of Okinawa indicating locations of Naha and Kadena AB. Elevations of selected peaks are in meters.

manually recorded on the hour. Winds from special surface observations, which were generally recorded between hours, are averaged vectorially to obtain the average wind direction, and algebraically to obtain the average wind speed for each hour. In the case of a single surface observation with a variable wind direction, the directional extremes are vectorially added to give an average direction.

Up to ten values of 6-minute profiler winds (u, v and w) are combined each hour to give a consensus of the winds aloft. Detailed discussion of this technique can be found in Lind (1993) and an abbreviated version in Section I above. Comparisons are made with both the corresponding hourly surface sustained wind and surface gusts.

1.   Predictor and Equation Selection

a.   Sustained Wind and Gusts

Consensus winds from the first five profiler range gates are included in the stepwise regression as potential predictors of the surface wind speed. Additional predictors for the surface gust prediction include the squares of the consensus wind speeds, and the spectral widths of the return echoes from each of the three beams. The spectral width is a measure (in m/s) of the broadness of the power distribution. These predictors were included because it had been observed that the spectral width increased in gusty conditions. Although a spectral width predictor could not be used with aircraft-measured upper-level winds, it may be a useful descriptor of boundary layer structure at the profiler site.

The spectral width of the return echo from an antenna beam depends not only on the character of the wind, but also the direction of the beam relative to the wind direction. The strongest signal is received when the beam points into or away from the wind. Since each beam points in a fixed direction, the

most sensitive beam will not be the same in every wind condition. With this in mind, five potential predictors are chosen--each a combination of the three beams at one level. A predictor is defined from the average spectral width of the three profiler beams for the first five wind profiler range gates.

Based on the scatter plots of surface sustained wind and gusts versus the profiler wind speeds (Figs. 7 and 8), linear and quadratic equations are derived to best fit the distributions. The best fit is defined as the model that had the smallest mean error, the smallest error variance (where "error" is the absolute value of the difference between the observed and predicted winds), and the largest explained variance (r-squared, where r is the correlation between the observed and predicted winds). The quadratic model ($Y = a + bX + cX^2$, where Y is the surface wind and X is the upper-level wind), is typically the best fit for gust data after eliminating the linear term bX. Since X is highly correlated with X^2 and the standard error of X is often only a factor of two smaller than the coefficient of X, valuable information is not lost by excluding this term.

The residuals (observed - predicted) for surface wind speed and surface gust (not shown) are randomly distributed about zero, which indicates the appropriateness of the respective models. Since the residuals are relatively small compared to the magnitude of the winds (68% of the wind speed errors and gust errors are within 0.94 m/s and 1.23 m/s, respectively, for a 600 m regression), confidence in the regression models is good.

Although the sustained winds tend to zero as the winds aloft tend to zero (Fig. 7), the surface gusts do not (Fig. 8). By definition, a gust is reported when fluctuations of 10 kt (5 m/s) or greater exist in the wind speed.
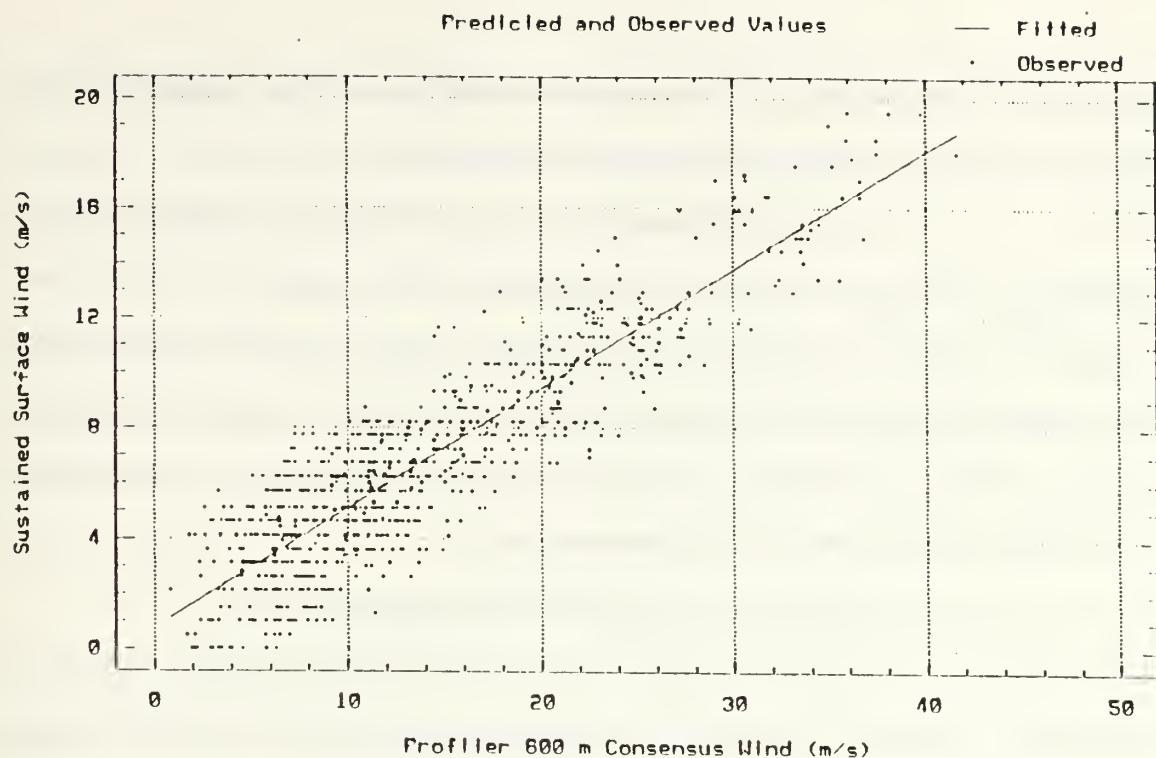
Fig. 7. Scatterplot of the 600 m wind speed versus the surface sustained wind speed (m/s). A least-squares linear fit to the data is given.
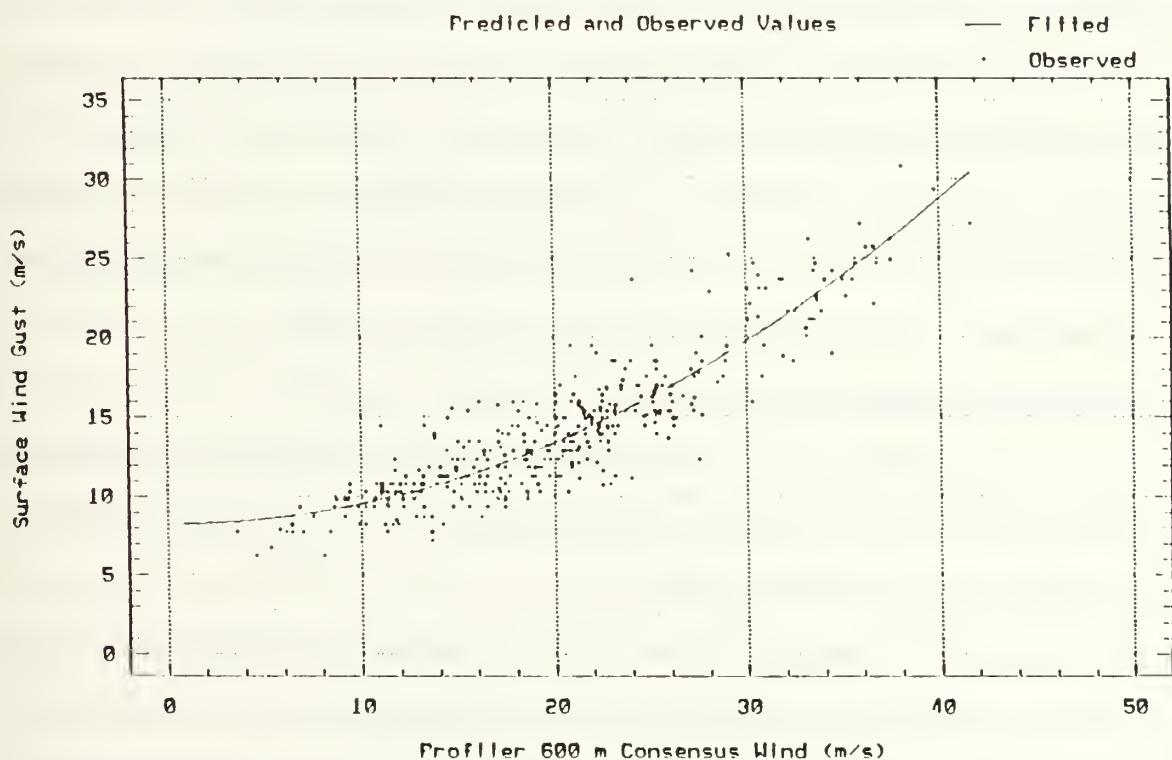
Fig. 8. Scatterplot of the 600 m wind speed versus the surface wind gust (m/s). A least-squares quadratic fit to the data is given.

27

Because this requirement can never be met with light surface winds, the gust observations should not be expected to tend toward zero.

In the upper-level wind range of 10-25 m/s (compare Figs. 7 and 8), the surface gusts are about 4 m/s greater than the sustained winds. Above 25 m/s, the surface gusts increase more rapidly than do the sustained winds. For example, a wind profiler observation of 40 m/s would be expected to have a sustained surface wind of 18 m/s (about 45% of the upper-level wind) and a surface gust of 28 m/s (about 70% of the upper-level wind).

b.   Predictive Equations for Wind Speed and Gusts

Several methods for predicting the surface wind are investigated. The first method allows comparisons with Powell (1982) and Powell *et al.* (1991) in that mean ratios of the surface winds to the upper-level winds are computed for each of the five levels. These ratios are derived for potential application to aircraft or satellite upper-level winds as a reduction factor to predict surface winds. In a second approach, least-square regressions are derived with several combinations of predictors. A predictive equation is calculated and tested for each of the five lowest wind profiler levels. At the very least, a regression equation has superior predictive ability (compared to ratios) if the regression produces an equation with a non-zero intercept. Not only are five predictive equations cumbersome, the choice of the most appropriate equation to predict the surface wind may not be obvious when the upper-level wind does not come from exactly 600, 900, 1200, 1500 or 1800 m.

To determine the magnitude of the prediction error that would result if the upper-level wind did not come from exactly one of the five levels, the best of the five predictive equations (as judged by having the highest r-squared and

28

lowest mean error and error variance--see Section B.1.a.) is used with winds from each level. The prediction errors were then compared with those from the five predictive equations to see how much the forecast is degraded.

Lastly, since the single best predictive equation is generally derived from the winds closest to the ground (600 m), the equation may be inadequate for winds from levels far above the surface. This possibility is addressed by calculating a mean-layer wind (600 - 1800 m) and using it as a predictor of the surface condition.

Kolmogorov-Smirnov (K-S) tests are performed with the errors (predicted - observed) from various equations to test whether the errors from one equation are significantly different from those of another equation. Unlike the common t-test, which tests if the means are significantly different, the K-S test uses the cumulative distribution of the errors to test if the errors are significantly different. Critical values are calculated for 95% significance levels (alpha = 0.05). If the critical value is 0.05 or greater, then the equations are not significantly different. Statistics from all investigations are calculated using winds from each level as input into the equations (Appendix B).

c.   **Sustained Wind Direction**

Although the surface wind direction prediction also uses relationships derived from winds from the surface through 1800 m, the direction prediction departs from the wind speed and gust prediction in that a regression technique is not used for the direction prediction. Instead, consensus winds from the first five profiler range gates are used in a statistical sense to determine the degree that the wind direction shifts as the distance above ground increases. Knowing the directional difference between range gates allows the surface wind

29

direction to be obtained from a wind direction in the boundary layer. To compute the average wind direction shift between levels, first a "shifted" vertical wind profile was made. The 600 m wind direction was rotated to 090 degrees. In doing so, the number of degrees that the wind direction was shifted was noted. Next all other wind directions (surface, 900, 1200, 1500 and 1800 m) are shifted the same amount. Thus, all wind directions are represented relative to a 600 m wind direction of 090 degrees. The mean wind shift was obtained between levels by averaging the "shifted" directions at a particular level and for each level.

Because friction is not linear with height, the change in wind direction with height also is not linear, as shown by a hodograph of the average "shifted" wind direction (Fig. 9). The average surface wind direction is always counterclockwise from the upper-level wind direction. Conversely, the upper-level wind direction is shifted clockwise from the surface wind direction. This effect is expected because friction makes the surface wind subgeostrophic.

2.   **Data Stratifications**

As indicated in Fig. 6, the profiler was located on the west coast of Okinawa. In general, winds from 215 to 330 degrees represent an over-sea trajectory and the remainder of the winds have a trajectory over land. However, scatter plots of surface versus upper-level wind direction (Fig. 10) indicate winds with directions from 220° clockwise to 360° may be a better description of winds with over-water trajectories. Due to the differences in heat fluxes and momentum transfer over land versus over the sea, separating data into winds influenced by either land or sea seemed to be an obvious way to improve on the regression models derived from all of the data.
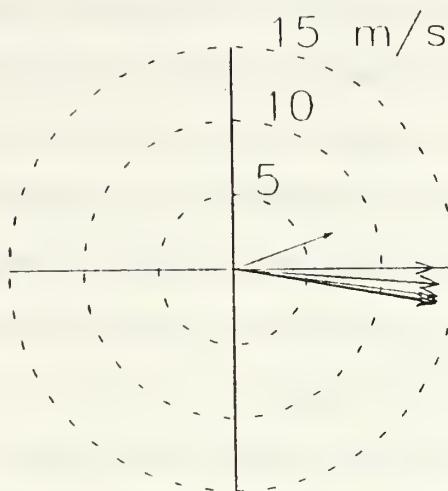
Fig. 9. Hodograph of average wind direction "shifted" relative to the 600 m wind direction oriented toward 90°. The wind directions and speeds (m/s) from the surface to 1800 m are 070/07, 090/14, 094/14, 098/14, 099/14 and 100/14.
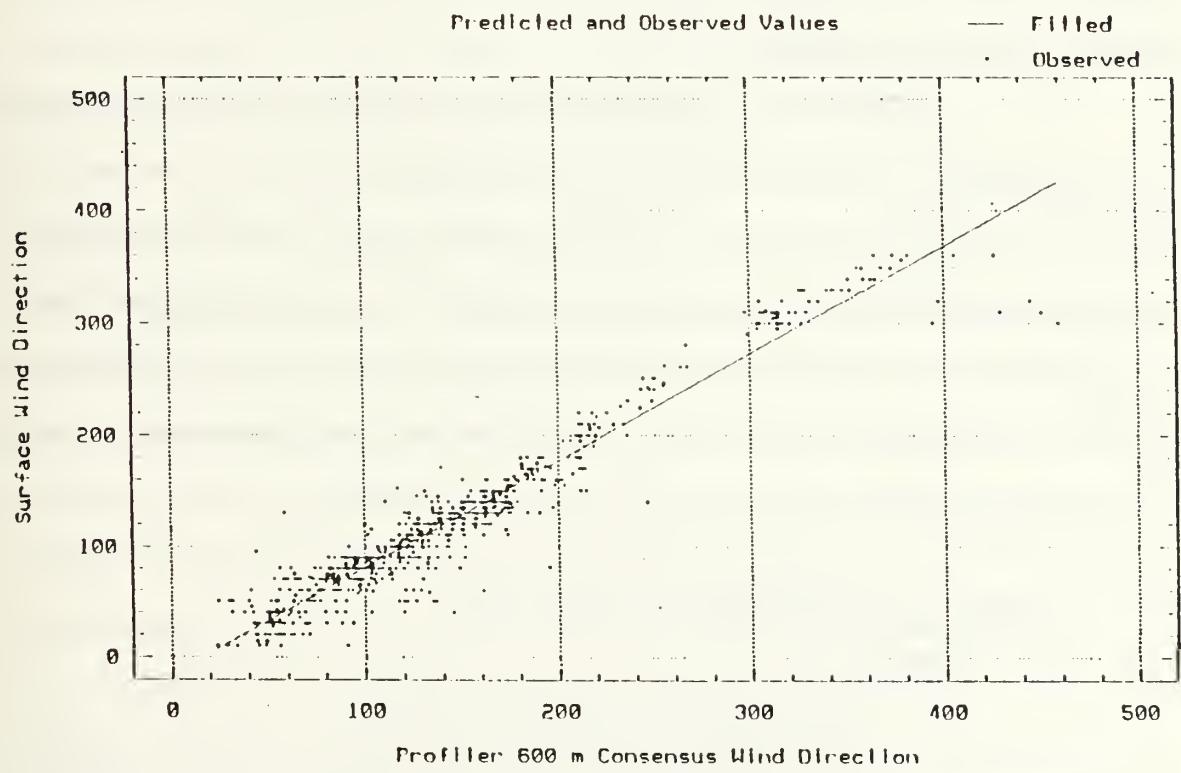
Fig. 10. Scatterplot of the 600 m wind direction (abscissa) versus the surface wind direction (degrees).

Diurnal effects may also play a role in the prediction of the surface wind. Consequently, the data set is also stratified into subsets of day and night. During the 44 days of profiler operation at Okinawa, sunrise changed by about 15 minutes, and sunset by about 45 minutes. Because of the small variations in these times relative to the long duration of diurnal forcing, average times of 2100 UTC for sunrise and 0900 UTC for sunset are deemed adequate to separate hours of day and night. To cleanly delineate day and night data, observations from the hours of 0900 and 2100 are not included in either subset.

Profiler observations with 600 m wind speeds less than 2.6 m/s are removed from the land/sea stratifications. In addition, wind observations that had less than 2.6 m/s at any level are removed from the wind direction prediction data because typically the surface winds for these cases are light and variable and therefore difficult to predict.

In addition to the stratifications described above, wind direction data are also stratified with respect to the 600 m wind speed. This is done because wind direction is highly dependent on friction, and friction is a function of wind speed. Two stratifications are tested: weak (less than 13.4 m/s), and strong (greater than or equal to 13.4 m/s). The 13.4 m/s cutpoint is chosen as it is the mean 600 m wind speed. The average surface wind that corresponds to each stratification is approximately 5 m/s for the weak, and 10 m/s for the strong.

C.   SURFACE WIND PREDICTION RESULTS

1.   All Data

a.   Lower-level/Upper-level Wind Ratios

Simple ratios first are computed for each of the 1022 paired (surface to upper-level) sustained wind observations and for each of the five range

gates (Table 3). The best ratio for predicting the surface wind is 0.517 times the 600 m wind, which gives a mean error of 1.49 m/s and an error standard deviation of 1.04 m/s. It is no surprise that winds from the profiler level closest to the surface are most highly correlated with the surface wind. It is interesting that the worst surface wind prediction (mean error 1.83 m/s, error standard deviation 1.42 m/s) uses winds from the 1500 m range gate (and not a higher gate). This indicates a nonlinear wind speed versus height relationship in the boundary layer, and the maximum ratio for 1500 m indicates the average minimum wind speed for the layer is at 1500 m. Within the 600 to 1800 m layer, a reduction factor between 0.517 and 0.542 best approximates the surface sustained wind speed. These results compare favorably with the reduction ratios derived in the Powell aircraft observations of hurricane winds over terrain (Table 2). K-S tests (Appendix B) between the 600 m prediction errors and those at other levels indicate the errors at all levels except 900 m are significantly different (alpha = 0.05) from those at 600 m.

Wind ratios relating the upper-level wind to the surface gusts range from 0.713 for 1200 m to 0.736 for 600 m (Table 3). Unlike the sustained wind ratios, the gust ratios yield prediction errors that are not significantly different at the five levels. As with the sustained wind prediction, the lowest level (600 m) gives the most accurate prediction of the surface gust (with a mean error of 2.10 m/s and error standard deviation of 1.43 m/s). Ratios from the highest levels (1200 - 1800 m) are the least accurate for predicting the surface gust. The ratio derived from the 1200 m wind increases the mean error 0.23 m/s, while the largest increase in error variance (with respect to the 600 m level) occurs with the 1800 m wind ratio (0.30 m/s). As was the case with the surface sustained wind ratios described above, the gust ratios are within one standard deviation of the Powell et al. (1991) ratios.

TABLE 3. SURFACE WIND PREDICTION RATIOS AND PREDICTION ERROR STATISTICS FOR 1022 PAIRED OBSERVATIONS OF SURFACE AND UPPER-LEVEL WIND. The mean and standard deviation apply to the absolute value of the prediction minus the observed surface wind. The wind speed at each level multiplied by the ratio for that level predicts the surface wind speed (units m/s).

Height (m)	Sustained Wind Ratio	Prediction Error Mean	Prediction Error St.Dev.	Gust Ratio	Prediction Error Mean	Prediction Error St.Dev.
600	0.517	1.49	1.04	0.736	2.10	1.43
900	0.522	1.65	1.23	0.717	2.29	1.66
1200	0.522	1.72	1.31	0.713	2.33	1.72
1500	0.542	1.33	1.42	0.715	2.29	1.72
1800	0.536	1.76	1.34	0.721	2.28	1.73

b. Surface Wind Prediction With Linear Regression

Least-square regressions are derived to estimate sustained surface winds from the winds at each of the upper levels as predictors (Table 4). As with the sustained wind ratios above, the 600 m wind is the best predictor of the surface wind (mean error 1.37 m/s, standard deviation 0.94 m/s). The higher altitude winds provide only slightly less accurate predictions. A simple linear regression equation of 0.433 times the 600 m wind plus 0.77 best specifies the surface wind. The regression equation technique reduces the prediction errors compared to the above ratios approach by 0.12 m/s (for the 600 m predictor) to 0.43 m/s (for the 1500 m predictor). Likewise, the error standard deviations are reduced 0.10 and 0.40 m/s for the same levels. Thus, the regressions provide a modestly better relationship between the upper-level and surface winds than the simple ratios as used by Powell.

Five equations (each one for a specific level) do not make a satisfying model. For example, which equation should be used if the upper-level wind altitude does not match one of the levels that were used to derive the equations? The most desirable model for surface wind prediction would be a single equation that would give valid results if provided input from any level in a specified layer. Such a single equation approach will be tested in Sections c. and d. below.

Initially, the predictive power of the spectral widths is tested by using spectral widths from each of the first five range gates as potential predictors of the surface gust. The best spectral width predictors for the surface gust (with a r-squared of 55.6%) is a combination of the average spectral widths from 600 and 1500 m (not shown). Since the spectral widths alone do not satisfactorily predict the surface gusts , the pool of potential predictors is increased to include wind speeds

TABLE 4. SURFACE WIND REGRESSION EQUATIONS AND PREDICTION ERROR STATISTICS FOR 1022 PAIRED OBSERVATIONS OF SURFACE AND UPPER-LEVEL WIND. The wind speed (in m/s) at each level when substituted for X in each equation will predict the surface wind speed. Equations for each level were derived from data at that level. The mean and standard deviation apply to the absolute value of the prediction minus the observed surface wind.

Height (m)	Sustained wind = a + b X		Gust = a + b X + c X²		
	a	b	a	b	c
600	0.77	0.433	8.27	.0	0.0128
900	1.11	0.398	8.56	.0	0.0111
1200	1.19	0.389	8.59	.0	0.0108
1500	1.20	0.391	8.53	.0	0.0111
1800	1.18	0.395	8.53	.0	0.0114

Height (m)	R-Squared Sustained / Gust	Sustained Wind Prediction Error		Wind Gust Prediction Error	
		Mean	St.Dev.	Mean	St.Dev.
600	.80 / .82	1.37	0.94	1.45	1.23
900	.79 / .79	1.39	0.97	1.52	1.33
1200	.79 / .79	1.40	1.00	1.52	1.35
1500	.78 / .79	1.40	1.01	1.53	1.39
1800	.78 / .79	1.41	1.01	1.57	1.34

and squares of wind speeds from the five lowest profiler gates. The best surface gust prediction equation includes not only the 600 m wind spectral width average, but also the 1800 m wind and the square of the 600 m wind as the predictors. This combination results in a r-squared of 82.7%. Since the 1800 m wind and the 600 m spectral width together add only 1% to the r-squared, these predictors are removed from the predictive equation, and the regression is run with only the 600 m wind squared as the "best" predictor.

The resultant second-order equation based on the 600 m data provides a good fit for the surface gust reports (Table 4). Compared to the predictions using the ratios approach (Section a. above), regression equations for each level reduce the mean prediction errors between 0.65 and 0.81 m/s, and the error standard deviations between 0.20 and 0.39 m/s. As with the sustained wind prediction, the regression equation technique is superior to the ratios approach for predicting surface gusts, especially because of the non-zero intercept (Fig. 8).

c.   **Single Level Regression Error Statistics**

The discussion in Section b (above) showed that the equation that most accurately predicted sustained surface winds was a linear regression with the 600 m wind as the predictor. It is useful to document the magnitude of the errors expected if the input wind is not from 600 m. As an example, how much will the error in the surface wind prediction increase because the cumulus cloud-drift wind estimate from satellite imagery had an erroneous elevation attributed to it? The other four upper-level winds from 900 to 1800 m are entered into the best surface sustained wind prediction equation that was derived from the 600 m winds (Table 5). The mean errors and error variances for input winds from the four levels indicate a surprisingly small degradation in the prediction when compared to the

errors observed when using equations for the individual level (Section b above). Only about a 0.03 m/s increase in mean sustained surface wind error is found when a wind from a level other than 600 m is used as input to the 600 m regression equation (as opposed to using the specific regression equation derived for that particular level). Similarly, a very small increase (about 0.03 m/s) in the error standard deviation is found. The average of the mean errors from the four levels not used to derive the equation is 1.43 m/s, and the average error standard deviation is 1.03 m/s. That is, not only are the prediction errors small, but little difference is observed between predictions if the input wind is from a level other than 600 m. In addition, all of the mean errors and error variances from the single regression equation (Table 5) are smaller than those associated with the ratios approach computed for each level (Table 3). Based on these results, a single predictive equation, to be used with all levels, appears to give favorable predictions because not much vertical shear exists between 600 m and 1800 m (Fig. 9).

Gust prediction using the 600 m regression equation with winds from other levels (Table 5) increases the mean error a minimum of 0.05 m/s to a maximum of 0.14 m/s compared to the prediction errors from the individual regression equations (Table 4). Likewise, the increase in the error standard deviation is also quite small (0.10 - 0.18 m/s). As with the sustained surface wind prediction, using a single equation with winds from any level from 600 to 1800 m to predict the surface gust does not seriously degrade the forecast.

d.   Surface Wind Regression With a Mean-layer
        Wind

Powell (1982) composited upper-level winds from a 500 to 1500 m layer. For comparison, a regression based on a mean-layer wind from 600 to 1800 m is derived. Winds from the first five levels are added with equal weighting

(20%), and this layer average is then used as the predictor for the surface sustained wind speed. The resulting linear regression equation has 0.406 for the slope and 1.02 as the intercept. Mean errors and error variances of the predictions when using the wind from each of the first five levels as the input to this equation are shown in Table 6. Compared to predictions from the ratios approach (Table 3), the greatest improvement in predictability occurs when the input winds are from higher altitudes (1500 and 1800 m). For these levels, the mean error is reduced 0.42 and 0.35 m/s by using the mean-layer regression, and the error standard deviation is reduced by 0.40 and 0.33 m/s.

It is not surprising that the mean wind regression equation is superior to the ratios computed for each level (Section a. above, and Table 3). However, it is noteworthy that the degradation in the forecast accuracy, when compared to the five individual regression equations (Table 4) is negligible. A comparison between the error statistics from the single mean-layer equation (Table 6) and those from the five regression equations (Table 4) shows a very slight (0.01 m/s) increase in the mean error and error variance for all levels except the 600 m (standard deviation increase was 0.02 m/s). Therefore virtually no change in the predictability of the surface sustained wind is found when comparing the most accurate prediction equations (for each level) to the single predictive equation derived from the mean of the lowest five levels.

Gust prediction using the single regression equation derived from the square of the mean-layer (600 - 1800 m) wind also proved to be the best alternative to using the five individual regression equations. The largest increase (0.04 m/s) in the mean prediction error occurs at 600 m, and all other mean errors are 0.02 m/s and less. The largest increase in prediction error standard deviation

TABLE 5. PREDICTION ERROR STATISTICS FOR THE BEST (600 M) REGRESSION EQUATION. Statistics are for predictions using the 600 m equation with winds (in m/s) from other levels. Sustained wind = 0.77 + 0.433 x Upper-level Wind. Gust = 8.27 + 0.0128 x (Upper-level Wind)^2. The mean and standard deviation apply to the absolute value of the prediction minus the observed surface wind.

Height (m)	R-Squared Sustained / Gust	Sustained Wind Prediction Error		Wind Gust Prediction Error	
		Mean	St.Dev.	Mean	St.Dev.
600	.80 / .82	1.37	0.94	1.45	1.23
900	-- / --	1.41	0.99	1.61	1.45
1200	-- / --	1.44	1.03	1.66	1.52
1500	-- / --	1.43	1.05	1.65	1.51
1800	-- / --	1.43	1.03	1.62	1.45

TABLE 6. PREDICTION ERROR STATISTICS FOR THE MEAN-LAYER REGRESSION EQUATION. Statistics are for predictions from equations derived from an average of the winds at five levels. Sustained wind = 1.02 + 0.406 x Upper-level Wind. Gust = 8.39 + 0.0116 x (Upper-level Wind)^2. The mean and standard deviation apply to the absolute value of the prediction minus the observed surface wind in m/s. The R-squared for the sustained wind and gust equations are 0.80 and 0.81 respectively.

Height (m)	Sustained Wind Prediction Error		Wind Gust Prediction Error	
	Mean	St.Dev.	Mean	St.Dev.
600	1.37	0.95	1.49	1.31
900	1.39	0.97	1.52	1.34
1200	1.41	1.00	1.53	1.37
1500	1.41	1.01	1.55	1.39
1800	1.41	1.01	1.56	1.35

(0.07 m/s) also occurs at 600 m, which is followed by 0.03 m/s at 1200 m, and 0.01 m/s or less at the other levels. Since these differences are so small, there is clearly great merit to using this single-layer equation for predicting surface gusts.

e.   **Surface Wind Direction Prediction**

The hodograph of the average wind at each of the six levels (Fig. 9) has a 20 degree clockwise rotation of the wind from the surface to 600 m and an increase in wind speed from 7.2 to 13.6 m/s. The wind continues to veer (eight degrees) in the next 600 m, and the wind speed becomes constant at 14 m/s. Above 1200 m, the upper-level wind direction is 30 degrees clockwise from the surface wind direction and the upper-level wind speed is about two times greater than the surface wind speed.

Stratifying the data into two classes based on the 600 m/s wind speed (weak, < 13.4 m/s and strong, > 13.4 m/s) allows wind direction dependency on wind speed to be assessed. When using all of the data, no statistically significant relationships are apparent. That is, the wind shifts from gate to gate are essentially the same regardless of whether the wind is "weak" or "strong" (Figs. 11 and 12).

f.   **All Data Investigation Summary**

Analysis of the entire data set revealed that surface sustained wind speed is well represented by simple linear equations (Table 4). Due to a nonlinear relationship with the upper-level winds (Fig. 8), wind gusts are better predicted by the square of the upper-level wind speed (Table 4). A simple ratio of the surface wind to the upper-level wind (which is equivalent to assuming a zero intercept in the regression equation) provides a less accurate prediction of the surface condition. However, these wind ratios are useful for comparison with studies such as Powell (1980, 1982), and Powell *et al.* (1991), and understanding
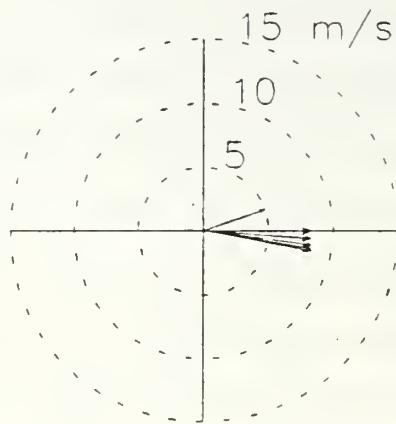
Fig. 11. As in Fig. 9, except for 600 m wind speeds less than 13.4 m/s. The wind directions and speeds from the surface to 1800 m are 070/05, 090/08, 094/08, 097/09, 099/09 and 101/09.
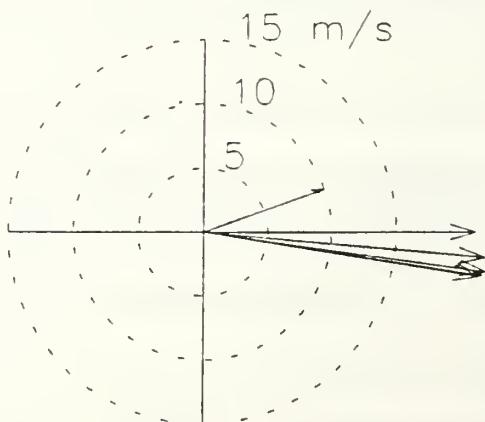
Fig. 12. As in Fig. 9, except for 600 m wind speeds greater than 13.4 m/s. Wind directions and speeds from the surface to 1800 are 070/10, 090/21, 095/22, 098/22, 099/22 and 099/22.

relationships between the winds aloft and those at the surface. If an upper-level wind speed is known to be at a level near 600 m, the 600 m regression equation will give the best prediction of the surface condition (Table 4). For an input wind from levels between 900 and 1800 m, satisfactory results can be obtained by using the mean-layer regression equations for wind speed and gust (Table 6).

The results of this investigation show that mean wind speeds and gusts can be nicely described by regression equations. However, it should be noted that upper-level wind data when plotted against the surface wind (Figs. 7, 8 and 10) reveal large scatter about the mean. As a consequence, improving the prediction of a surface parameter by selecting a regression equation for a specific level because it has a slightly larger r-squared or smaller mean error is not necessary. Large error variances confirm this. Additionally, the wind structure above 600 m changes little with height. For example, the wind speed differences at 300 m intervals are often less than 1 m/s, which illustrates that it is not necessary to choose an equation for one level over another. The mean wind direction shift from the surface through 1800 m is 30°, with almost all of this change occurring in the surface to 1200 m layer. The 900 m wind speed is about twice the 7 m/s mean surface wind speed. These profiler winds beginning at 600 m do not give an unambiguous definition of the depth of the boundary layer.

Because the mean-layer wind is a satisfactory predictor of the surface wind, only the wind ratio and mean-layer regression results will be discussed below. Although the individual level regression equations and prediction statistics for the stratifications were calculated, they will not be presented here as they do not add much additional information.

2. Day vs Night Data (Diurnal Effects)

a. Lower-level/Upper-level Wind Ratios

Stratifying the data set into day (Table 7) and night (Table 8) subsets shows that a higher percentage of the upper-level winds are found at the surface during the day than at night (i.e., about 63% for day and about 41% for night for sustained wind ratios using the 600 m level). This is consistent with the increase in turbulent kinetic energy resulting from a daytime upward sensible heat flux. As a consequence of this more turbulent regime, a larger range of surface wind speeds exists for a given upper-level wind. For example, larger mean errors and standard deviations are found for the daytime predictions (Table 7) than for the nighttime predictions (Table 8). When the daytime predictions are compared to the predictions that use all data (Section C.1. above), and Table 3) the average increase in the mean error is 0.53 m/s (over the five levels), and the average increase in prediction error standard deviation is 0.60 m/s. Because the nighttime data has smaller variance, both the mean error and error standard deviation decrease as compared to the whole data set (Tables 3 and 8). The reduction in the mean error ranges from 0.36 m/s for the 600 m wind ratios to 0.57 m/s for the 1500 m wind ratios, while the reduction in error standard deviation is between 0.17 and 0.44 m/s.

Kolmogorov-Smirnov tests (Appendix B) show that the prediction errors from the daytime ratios are significantly different (0.05 significance level) than the errors from the nighttime ratios. In addition, the errors from both the daytime and nighttime ratios are significantly different from those obtained from the ratios derived from the whole data set (Table 3).

Similar to the sustained wind results above, the ratios of the surface gusts to upper-level wind show that the day gusts (Table 7) are a higher

44

TABLE 7.   AS IN TABLE 3, EXCEPT FOR DAYTIME OBSERVATION
RATIOS.

Height (m)	Sustained Wind Ratio	Prediction Error		Gust Ratio	Prediction Error	
		Mean	St.Dev.		Mean	St.Dev.
600	0.633	1.91	1.65	0.784	2.32	1.74
900	0.628	2.15	1.80	0.762	2.45	1.85
1200	0.634	2.33	1.97	0.758	2.54	1.92
1500	0.660	2.56	2.14	0.761	2.45	1.88
1800	0.629	2.18	1.77	0.764	2.43	1.74

TABLE 8.   AS IN TABLE 3, EXCEPT FOR NIGHTTIME OBSERVATION
RATIOS.

Height (m)	Sustained Wind Ratio	Prediction Error		Gust Ratio	Prediction Error	
		Mean	St.Dev.		Mean	St.Dev.
600	0.411	1.13	0.87	0.673	1.64	1.20
900	0.424	1.18	0.92	0.660	1.94	1.43
1200	0.415	1.20	0.95	0.656	2.05	1.49
1500	0.430	1.26	0.97	0.657	2.00	1.59
1800	0.449	1.34	1.01	0.665	2.05	1.60

percentage of the upper-level wind (78% at 600 m) than the night gusts (67% at 600 m). The prediction trends are also similar to the sustained wind prediction trends. That is, the mean error and error standard deviations increase (0.15-0.22 m/s and 0.01-0.30 m/s) for the daytime gust prediction (when compared to the ratios derived from the whole data set in Table 3) and decrease (0.28-0.46 m/s and 0.13-0.23 m/s) for the nighttime predictions. Kolmogorov-Smirnov tests (Appendix B) show that for heights 1200 m and below, the prediction errors from the nighttime ratios are significantly different (alpha = 0.05) than the prediction errors from both the daytime ratios and the entire data set.

b. Surface Wind Regression with a Mean-layer Wind

Before examining the mean-layer wind regression, it is useful to first examine relationships between the surface and the 600 m winds. Over most of the range of wind profiler velocities, the sustained surface winds during the day are higher than the winds during the night (Fig. 13). The 97.5% confidence limits on the two regression curves are separate until the 600 m wind speed reaches approximately 30 m/s. That is, the mechanical mixing effects become so strong at higher wind speeds that diurnal effects become unimportant in the sustained wind prediction. The smaller nighttime values are expected as the nighttime stabilization over land and formation of nocturnal inversions tend to decouple the surface winds from the upper-level winds. This actually leads to a negative intercept in the regression for nighttime, which indicates the surface winds will fall to zero at night when the upper-level wind speeds are stronger than during the day (using 600 m winds as representative of the upper-level winds). The non-zero surface wind intercept for the day observations appears to be related to a significant number of surface winds that are equal to or greater than 600 m wind speeds in the range

46

0-8 m/s. This effect may be related to differential daytime heating in a shallow layer over land that sustains a surface wind across the coast.

Dividing the sustained wind data set into day (Table 9) and night (Table 10) observations improves the explained variance (r-squared) from 80% in the overall sample to 83% (day) and 85% (night), and reduces the layer-average prediction errors compared to the overall sample in Table 6. Improvement in the mean prediction error when using separate day and night equations instead of the single mean-layer equation falls between 0.18 and 0.25 m/s (day) and 0.11 and 0.27 m/s (night). Although these improvements are small, they are all statistically significant (alpha = 0.05) except those for levels that are 1200 m and above (night) and 1800 m (day) (Appendix B).

Stratification of the surface gust data into night and day subsets significantly improves only the daytime predictions relative to a combined sample (Tables 6, 9 and 10). Although the 600 m daytime gust prediction error and standard deviation (Table 9) are only hundredths of a m/s greater than those from the overall mean-layer equation (Table 6), Appendix B suggests that the distribution of errors from these two equations are statistically significant. This apparent discrepancy is resolved with the understanding that the prediction statistics in the tables are computed from the absolute values of the errors, whereas the Kolmogorov-Smirnov statistics in Appendix B are based on the actual distribution of prediction errors (not an absolute value). In general, the daytime gust prediction errors are significantly different (smaller) than those from the entire data set because the daytime predictive equation is a full quadratic, and the equation derived from all data is a quadratic with the linear term removed.

47

TABLE 9. AS IN TABLE 6, EXCEPT FOR DAYTIME MEAN-LAYER EQUATION. Sustained wind = 2.25 + 0.379 x Upper-level wind. Gust = 6.53 + 0.220 x Upper-level Wind + 0.0069 x (Upper-level Wind)^2. The R-squared for both sustained wind and gust equations is 0.83.

Height (m)	Sustained Wind Prediction Error Mean	St.Dev	Wind Gust Prediction Error Mean	St.Dev.
600	1.19	0.85	1.46	1.32
900	1.17	0.85	1.41	1.30
1200	1.16	0.90	1.39	1.26
1500	1.16	0.89	1.36	1.21
1800	1.18	0.89	1.37	1.21

TABLE 10. AS IN TABLE 6, EXCEPT FOR NIGHTTIME MEAN-LAYER EQUATION. Sustained wind = - 0.14 + 0.432 x Upper-level Wind. Gust = 7.92 + 0.116 x (Upper-level Wind)^2. The R-squared for both sustained wind and gust equations are 0.85 and 0.82, respectively.

Height (m)	Sustained Wind Prediction Error Mean	St.Dev	Wind Gust Prediction Error Mean	St.Dev.
600	1.10	0.82	1.33	1.31
900	1.19	0.92	1.50	1.32
1200	1.21	0.95	1.63	1.45
1500	1.26	0.97	1.65	1.55
1800	1.30	0.98	1.66	1.49

Although the distributions of prediction errors for daytime and nighttime gusts are significantly different, the differences between the daytime and nighttime gusts (Fig. 14) is dependent on wind speed (using 600 m wind as an example). Significant differences do not exist between the surface gusts if the upper-level wind exceeds 30 m/s. However, nighttime surface gusts are less than daytime gusts if the upper-level winds are in the 15-30 m/s range. For profiler winds below 15 m/s, the curves in Fig. 14 are not significantly different. Little confidence can be placed in the curves at low speeds because no surface gusts were observed for profiler speeds below 9 m/s (4 m/s) during the night (day). Consequently, a general statement is that surface gusts at night will be smaller than day gusts for the same profiler wind speed, unless the upper-level winds are less than 15 m/s or exceed 30 m/s.

c. **Surface Wind Direction Prediction**

Comparing subsets of daytime and nighttime wind shift and speed data (Figs. 15 and 16) gives insight into the structure of the lower boundary layer. A daytime wind shift of about 30° (clockwise with height) occurs between the surface and 1200 m. From this height to 1800 m, the wind speed and direction are essentially constant at 14 m/s and 30° from the surface wind direction. Although the daytime surface to 600 m wind shift is the same (about 20°), the nighttime wind shifts above this height are smaller and the direction is not constant above 1200 m. The mean wind speeds for each of the levels are in agreement with the wind speed ratios (part a. above) in that they also indicate a larger fraction of the upper-level wind speed is reflected in the surface daytime wind speed when compared to the nighttime wind speed. The larger wind shifts during the day occur because the daytime surface heating destroys the nocturnal inversion and allows the surface

49
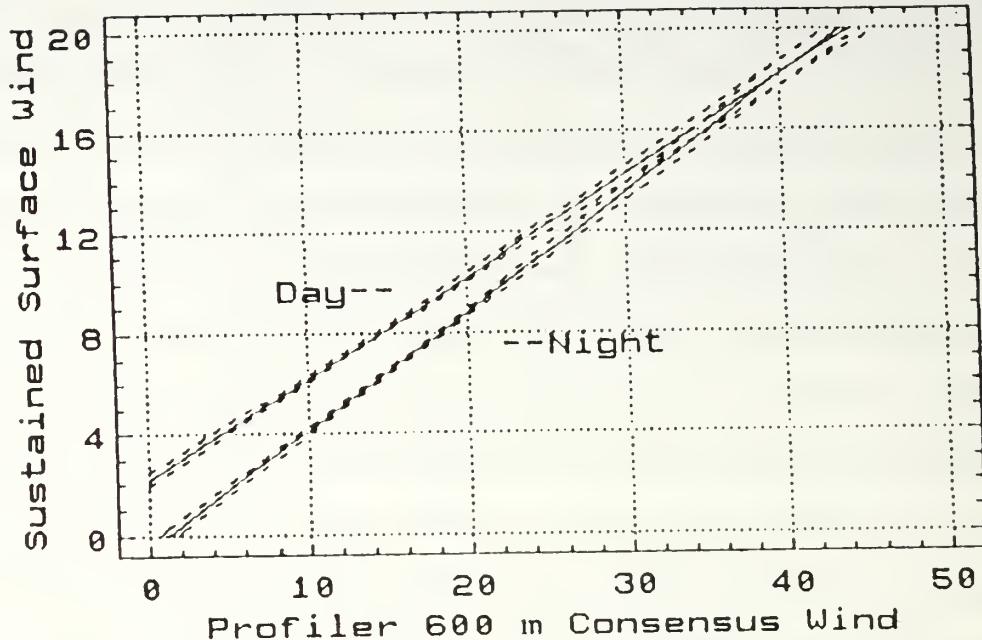
Fig. 13. Regression curves of the 600 m wind speed versus the surface sustained wind speed during the day and night. Dashed lines show 97.5% confidence interval for each fit.
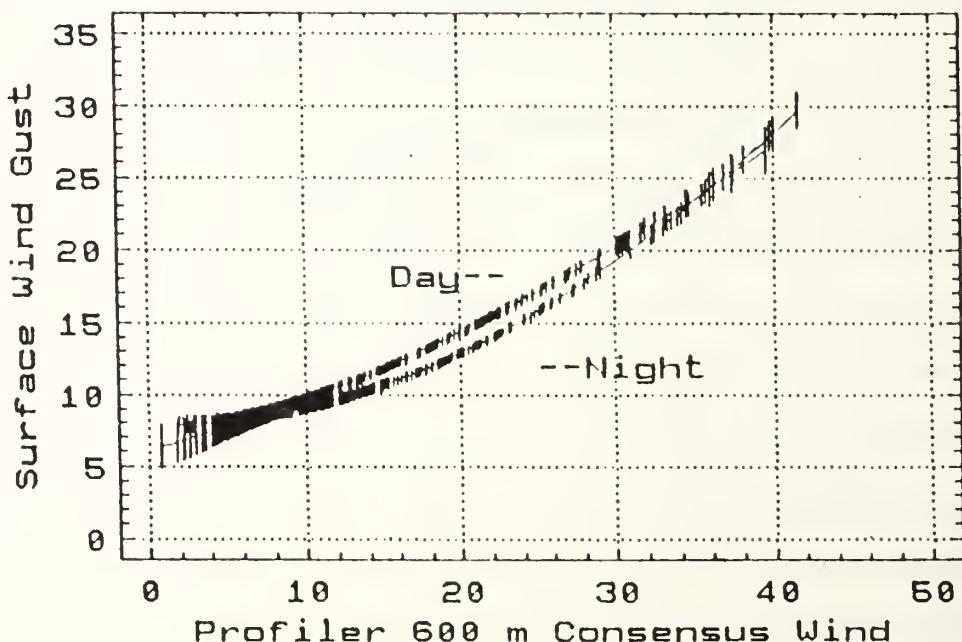
Fig. 14. Regression curves of the 600 m wind speed versus the surface wind gust during the day and night. Vertical line segments indicate 97.5% confidence levels along each curve.

50
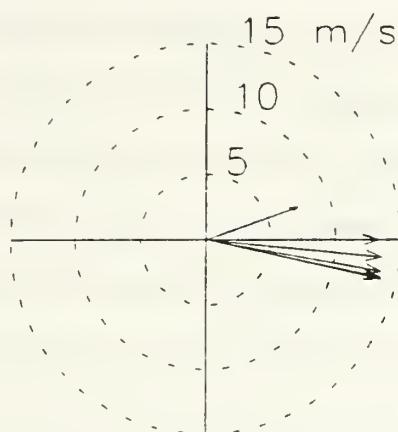
Fig. 15. As in Fig. 9, except for daytime winds. The wind directions and speeds from the surface to 1800 m are 071/08, 090/13, 096/14, 100/14, 103/14 and 102/14.
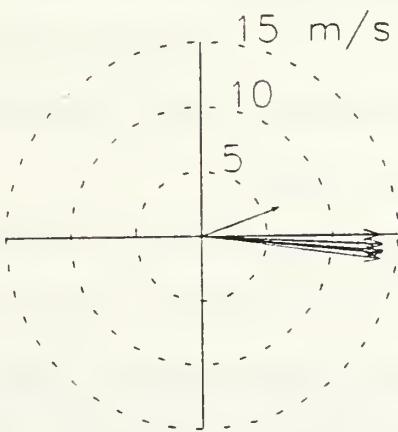
Fig. 16. As in Fig. 9, except for nighttime winds. The wind directions and speeds from the surface to 1800 m are 070/06, 090/14, 093/14, 095/14, 096/14, and 098/14.

winds to become less subgeostrophic by linking them with the upper-level winds (assumed to be nearly geostrophic).

The day/night data are further stratified into subsets of high and low 600 m wind speed (Figs. 17 and 18). Regardless of whether it is day or night, or the wind is strong or weak, the surface direction on average is 20° counterclockwise from the 600 m wind direction. As with the speed stratification results from the total data set, the night wind speed at the surface is weaker than the daytime surface wind speed and the winds aloft during the night are stronger than those during the day for the weak stratification. However, for the strong winds, the wind speeds at both the surface and aloft are greater during the day than during the night. This is consistent with more transport of momentum to the surface during the daytime in the absence of the nocturnal radiation inversion.

d.   Day vs Night Investigation Summary

The wind ratios reveal that a higher percentage of the upper-level winds are reflected in the surface sustained wind speeds and gusts: 63% (78%) for the daytime wind speed (gusts) and 41% (67%) for the nighttime wind speed (gusts). The ratios also have a larger variance in both the daytime sustained speeds and gusts. Because of this, only the nighttime ratios significantly improve the predictions of sustained wind speed and gusts, as compared to the predictions using the ratios derived from the total data set.

At low wind speeds and low altitudes, the day and night mean-layer regression equations are significantly different from the single equation derived from the total data set. Both the day and night sustained wind speed and prediction equations are improved with the day-night stratification. Only daytime gust predictions are significantly improved over the predictions from the equation
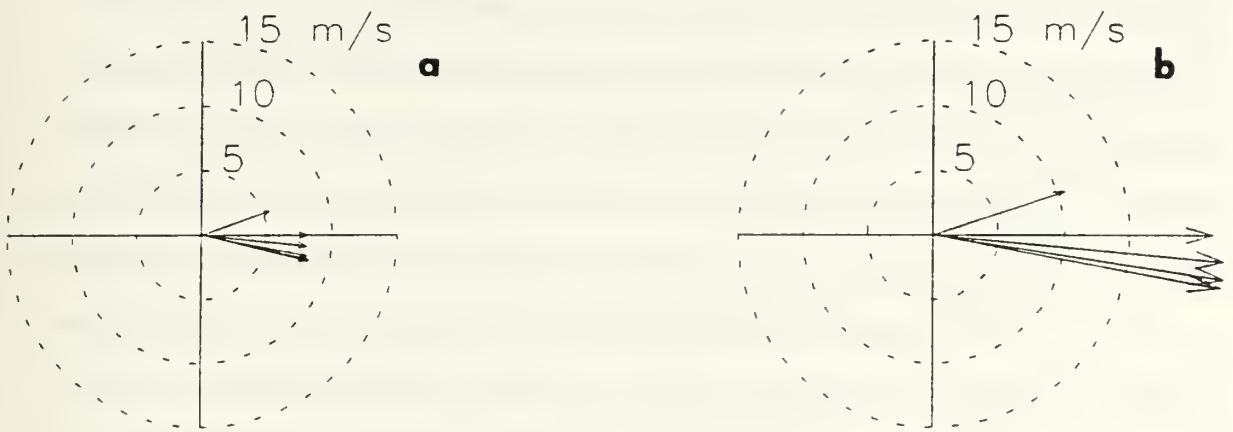
Fig. 17. (a) As in Fig. 9, except for daytime winds less than 13.4 m/s. The wind directions and speeds from the surface to 1800 m are 070/06, 090/08, 096/08, 101/08, 104/09 and 103/09. (b) As in Fig. 9, except for daytime winds greater than 13.4 m/s. The wind directions and speeds from the surface to 1800 m are 071/11, 090/21, 095/22, 099/23, 101/22 and 101/22.
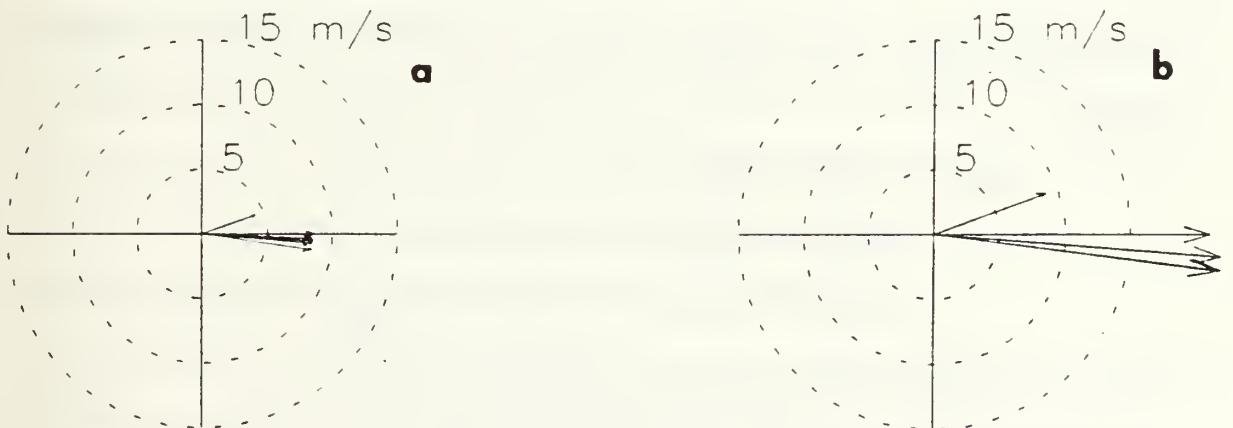
Fig. 18. (a) As in Fig. 9, except for nighttime winds less than 13.4 m/s. The wind directions and speeds from the ratios derived from the total surface to 1800 m are 070/05, 090/09, 092/09, 094/09, 095/09 and 098/09. (b) As in Fig. 9, except for nighttime winds greater than 13.4 m/s. The wind directions and speeds from the surface to 1800 m are 069/09, 090/21, 095/22, 097/22, 097/22 and 098/22.

derived from the entire data set. The confidence intervals demonstrate the daytime and nighttime gust equations have statistically significant differences when the upper-level wind is between 15 and 30 m/s. In a meteorological sense, the less than one m/s improvement over the mean-layer equation derived from all the data is not operationally significant. This applies to the sustained wind prediction as well. However, by examining the circumstances in which the stratifications are significant, insight into the structure of the boundary layer between 600 m and 1800 m is gained.

Wind direction shifts from the surface to 600 m are clockwise 20° for both night and day subsets. From 900 to 1200 m, the wind continues to veer an additional 10° in the daytime. Above 1200 m, the speed and direction are constant to 1800 m (the highest range gate used in this study). The nighttime data above 600 m continues to veer a total of 10° throughout the layer studied. Speed stratifications do not show a wind shift dependence on wind speed.

Tables with regression equations for the day and night data sets for each of the five lowest profiler range gates were also calculated, but they are not included as they have limited usefulness compared to the layer-average equations.

3.   **Land vs Water Trajectory Data**

a.   **Lower-level/Upper-level Wind Ratios**

As expected, ratios of surface to upper-level wind speed from winds with trajectories from over the water (Table 11) are larger than ratios derived from winds with land trajectories (0.526-0.555 m/s for water trajectories versus 0.510-0.546 m/s for land). Relatively smaller wind stresses over water surfaces allow the surface wind to maintain a higher speed than over the rough, solid land. However, this comparison is not really representative of the true land/sea contrast

because the profiler is 0.5 km from the water edge and the surface wind observation site is about 1.5 km farther inland.

Stratification of the entire data set into sea (Table 11) and land trajectory (Table 12) subsets significantly improves the prediction of the sustained surface wind when the profiler wind indicates a trajectory from the adjacent sea (about 0.5 km away). Errors from all levels except 900 and 1200 m were significantly smaller with respect to prediction errors from the total data set (Appendix B). Mean prediction errors and the error variances from the sea subset (Table 11) are less than those from the land subset (Table 12). The mean error is reduced by 0.28 m/s at 600 m and by 0.66 m/s at 1500 m, and the error standard deviation is reduced by 0.15 and by 0.56 m/s at the same levels.

Gust ratios at the five profiler range gates vary from 0.692 to 0.719 over land (Table 12) to 0.801 to 0.808 over water (Table 11). The larger ratios for sea trajectories are an indication that a greater percentage of the stronger upper-level winds make it to the surface. As with the land/sea stratification of the sustained wind, the stratification of the gust prediction equation reduces the prediction errors (mean and variance) of the sea subset in Table 11 (compared to the total data set in Table 3). However, Appendix B indicates that the reduction in the prediction errors is not significant at a 95% level of confidence.

b.   **Surface Wind Regression with a Mean-layer Wind**

Wind speed relationships between upper-level and sustained surface winds for the land and sea subsets are shown in Fig. 19. Although the 600 m wind is represented in this figure, similar relationships can be inferred between the surface and upper-level winds in general. Notice that the intercepts of the land- and sea-trajectory equations are nearly the same. Since the sea-trajectory sustained

TABLE 11. AS IN TABLE 3, EXCEPT FOR SEA OBSERVATION RATIOS.

Height (m)	Sustained Wind Ratio	Prediction Error Mean	St.Dev.	Gust Ratio	Prediction Error Mean	St.Dev.
600	0.537	1.21	0.89	0.811	1.75	1.50
900	0.544	1.36	0.94	0.807	1.88	1.51
1200	0.542	1.42	0.99	0.808	2.03	1.56
1500	0.526	1.17	0.86	0.801	1.70	1.36
1800	0.555	1.24	0.98	0.814	1.79	1.32

TABLE 12. AS IN TABLE 3, EXCEPT FOR LAND OBSERVATION RATIOS.

Height (m)	Sustained Wind Ratio	Prediction Error Mean	St.Dev.	Gust Ratio	Prediction Error Mean	St.Dev.
600	0.510	1.49	1.03	0.719	2.00	1.37
900	0.519	1.68	1.25	0.697	2.15	1.62
1200	0.520	1.75	1.34	0.692	2.18	1.65
1500	0.546	1.94	1.48	0.696	2.15	1.67
1800	0.536	1.83	1.36	0.701	2.14	1.66

wind slope is 0.49 versus 0.42 over land, the rough terrain of Okinawa (Fig. 6) has more of a damping effect on the sustained surface winds than the frictional effects of the sea surface (Fig. 19). The two regression equations are significantly different at a combined 95% confidence level when the upper-level speed is greater than 12 m/s (Fig. 19). At these higher speeds, the flow becomes more turbulent over the rough land surface, and the surface wind speed is reduced. By comparison, the flow at smaller wind speeds is relatively smooth over both land and sea, and the surface speed is not significantly different.

Because 90% of the profiler wind data have a wind direction from land, it is not surprising that the land-trajectory sustained wind equation (surface speed = 1.12 + 0.392 X upper-level wind speed) gives essentially the same prediction errors as the equation for the total set (Tables 6 and 13, Appendix B). Although the sea-trajectory equation (surface speed = 0.91 + 0.473 X upper-level wind speed) has an improved r-squared (values of 80 and 90% in Tables 6 and 14), the reduction in prediction error is not statistically significant when compared to the errors from the mean-layer equation derived from the whole data set (Appendix B). This startling result is probably because the "sea" subset actually has a land influence after crossing only 2 km of land to the surface observation site. Consequently, the contamination of the surface winds in the "sea" subset over this short distance means the winds are not as strong as they would be over open water, and the prediction errors from the land and sea subsets are not significantly different.

Similar land versus sea effects are present in the surface gust data. Although the land (Table 13) and sea (Table 14) equations are essentially identical at lower wind speeds, they are significantly different at higher speeds (Fig. 20). It is physically reasonable that the winds from the sea would be

TABLE 13.   AS IN TABLE 6, EXCEPT FOR LAND MEAN-LAYER EQUATION. Sustained wind = 1.12 + 0.392 x Upper-level Wind. Gust = 8.35 + 0.0111 x (Upper-level Wind)^2. The R-squared for both the sustained wind and gust equations are 0.79 and 0.82 respectively.

Height (m)	Sustained Wind Prediction Error		Wind Gust Prediction Error	
	Mean	St.Dev	Mean	St.Dev.
600	1.36	0.96	1.43	1.15
900	1.37	0.98	1.42	1.23
1200	1.38	1.00	1.43	1.27
1500	1.39	1.00	1.41	1.24
1800	1.38	1.00	1.44	1.16

TABLE 14. AS IN TABLE 6, EXCEPT FOR SEA MEAN-LAYER EQUATION. Sustained wind = 0.91 + 0.473 x Upper-level Wind. Gust = 8.50 + 0.0148 x (Upper-level Wind)^2. The R-squared for both the sustained wind and gust equations are 0.90 and 0.91 respectively.

Height (m)	Sustained Wind Prediction Error		Wind Gust Prediction Error	
	Mean	St.Dev	Mean	St.Dev.
600	1.18	0.86	1.47	1.34
900	1.17	0.88	1.36	1.17
1200	1.23	0.88	1.39	1.05
1500	1.12	0.88	1.46	1.01
1800	1.11	0.89	1.43	1.09

accompanied by larger surface gusts as well as larger sustained winds. However, the errors from the "land" and "sea" gust equations over all speeds are not significantly different (Tables 13 and 14, Appendix B).

c. Surface Wind Direction Prediction

The salient feature regarding the land/sea wind directional shift is the decreased wind shift from the surface to the 600 m level for winds with trajectories from over the water (9° versus 21° for over land) (Figs. 21 and 22). Although this wind shift is smaller, the wind speed is larger for the "sea" winds (8.9 m/s versus 7.0 m/s for over land). Both of these differences are obviously the result of decreased surface frictional effect over the short (2 km) distance from the water, which allows the surface wind to more closely approximate the geostrophic wind. Stratification of the land and sea data into winds less than and greater than 13.4 m/s (Figs. 23 and 24) shows a tendency for the wind shifts in the first 600 m of the "strong" subset to be slightly larger than those in the "weak" subset. However, the speed stratification indicates that, regardless of the wind speed, the clockwise wind shift from the surface wind direction to the 600 m wind direction remains about 12° greater for the land data.

d. Land vs Sea Trajectory Investigation Summary

The ratios of surface to upper-level wind speed and surface gust to upper-level wind speed from "sea" winds are larger than the ratios derived from "land" winds.

The separate ratios for "sea" data significantly improve the prediction of sustained surface wind at three of the five levels investigated. However, since there is not an appreciable difference between the "land" data and
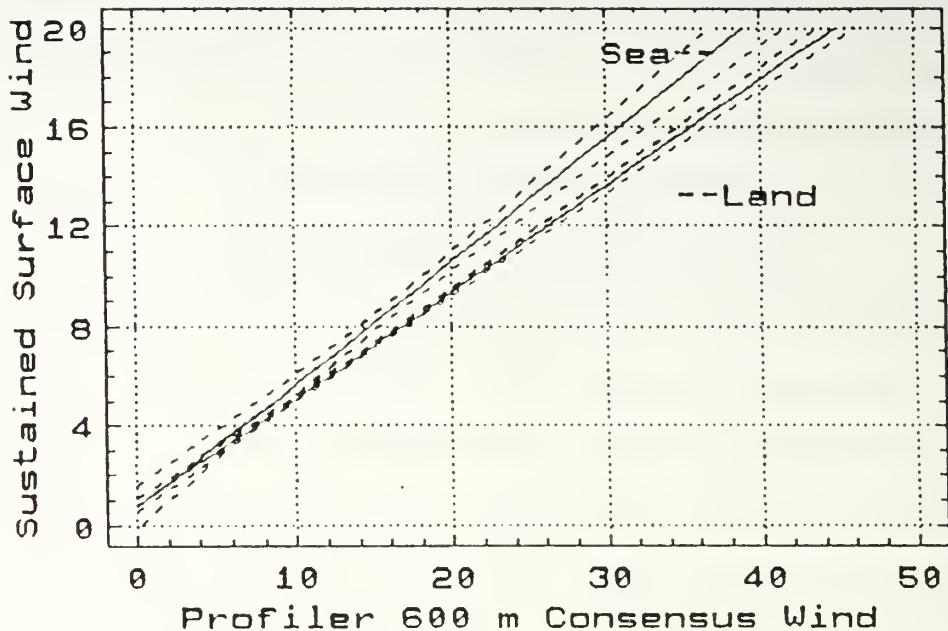
Fig. 19. Regression curves of the 600 m wind speed versus the surface wind speed for winds with trajectories from the sea or from the land. Dashed lines show 97.5% confidence interval for each fit.
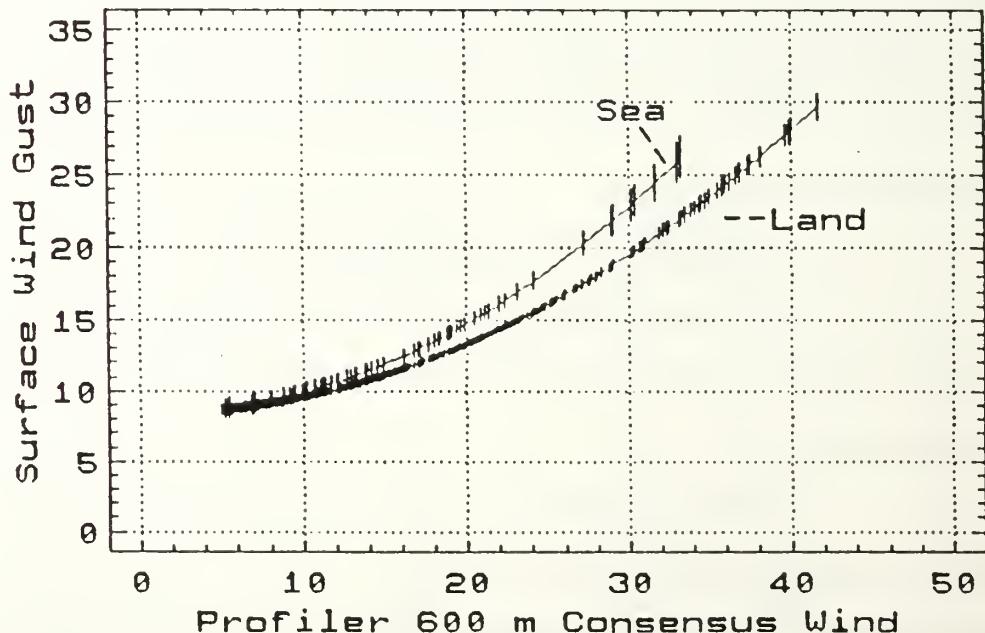
Fig. 20. Regression curves of the 600 m wind speed versus the surface wind gust for winds with trajectories from the sea or from the land. Vertical line segments indicate 97.5% confidence levels along each curve.
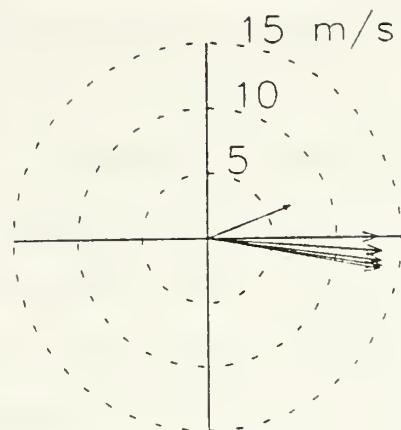
Fig. 21. As in Fig. 9, except for winds with trajectories from the land. The wind directions and speeds from the surface to 1800 m are 069/07, 090/13, 095/14, 098/14, 099/14 and 101/14.
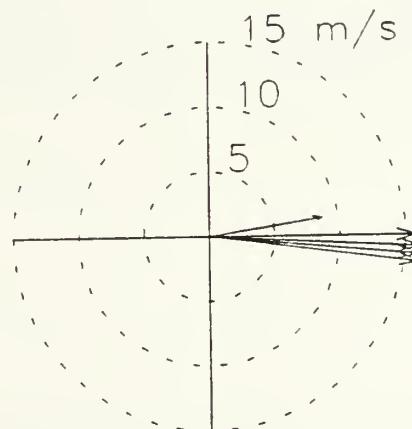
Fig. 22. As in Fig. 9, except for winds with trajectories from the sea. Wind directions and speeds from the surface to 1800 m are 081/09, 090/16, 093/16, 098/16, 097/16 and 095/16.

Fig. 23. (a) As in Fig. 9, except for winds less than 13.4 m/s and with trajectories from the land. The wind directions and speeds from the surface to 1800 m are 069/05, 090/08, 094/08, 097/08, 100/08 and 101/08. (b) As in Fig. 9, except for winds greater than 13.4 m/s and with trajectories from the land. The wind directions and speeds from the surface to 1800 m are 069/10, 090/21, 095/22, 098/22, 099/22 and 100/22.
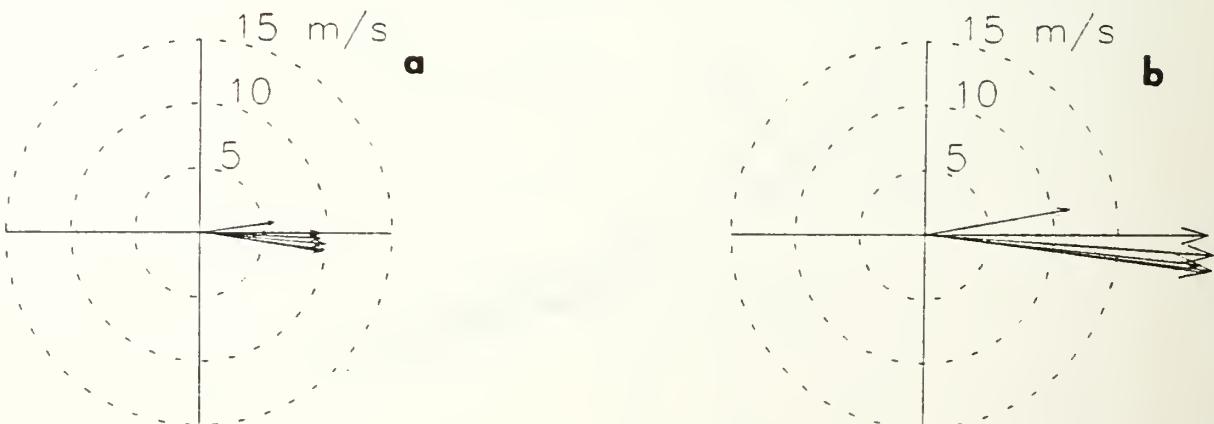
Fig. 24. (a) As in Fig. 9, except for winds less than 13.4 m/s and with trajectories from the sea. The wind directions and speeds from the surface to 1800 m are 082/06, 090/10, 092/10, 098/10, 097/10 and 095/10. (b) As in Fig. 9, except for winds greater than 13.4 m/s and with trajectories from the sea. The wind directions and speeds from the surface to 1800 m are 080/12, 090/22, 094/23, 097/23, 098/22 and 096/22.

the entire data set (90% of total data set was in the land subset), the prediction errors of the overall sample are not significantly reduced.

The mean-layer equations for land and sea data give essentially the same prediction errors as the equation for the total set (for both sustained surface wind and gusts). Although the r-squared is improved almost 10% with the sea stratification, the reduction in prediction error is not statistically significant.

Regression curves show that the difference between the surface winds over the sea and land is dependent on the upper-level wind speed. Both land and sea sustained winds and gusts are significantly different if the upper-level winds are stronger than 10 m/s.

Reduced drag over water allows the surface wind direction and speed to more closely match the upper-level wind. The average wind direction shift in the first 600 m above the surface is 9° for winds over water and 21° for winds over land.

Tables with regression equations for the land and sea data sets for each of the five lowest profiler range gates were also calculated, but they are not included as they have limited usefulness compared to the layer-average equations.

IV. CONCLUSIONS AND RECOMMENDATIONS

The key question addressed in Part II is whether microwave radar wind profilers would be a good way to increase the density of wind observation sites in the tropics. Although the start-up cost is large, the profiler needs minimal maintenance and requires no expendables such as balloons, gas and rawinsondes. The correlation between the rawinsonde and the radar wind profiler data is found to be 96% and better. This translates to 2 m/s differences in the u- and v-components. These figures are similar to those found by May (1992) for a rawinsonde-radar wind profiler study at Saipan during TCM-90.

Additional trends concerning the rawinsonde and profiler winds are observed. The median wind speed differences do not change as the wind speed increases, and the distribution of differences is rather narrow. Although more than one half of the comparisons are between ± 1.5 m/s, larger deviations exist when the wind speed is above 12.5 m/s. When the winds below 3315 m are stronger than 25 m/s, the wind speed differences have larger variances compared to other heights.

In summary, the wind profiler/rawinsonde comparisons in Part II demonstrate that the accuracy of the radar wind profiler as a wind measuring system is adequate for tropical sites. However, the 404 MHz profiler did not achieve observations throughout the troposphere, which would be required if the profiler was to replace the rawinsonde in the tropics.

In Part III, regression analysis shows that the surface sustained wind speed is well represented by simple linear equations. However, nonlinear equations provide a better relationship between the upper-level wind and the surface gusts. Although a simple ratio of the surface wind to the upper-level wind provides a less accurate

prediction of surface winds, the ratios agree well with those described by Powell (1980, 1982) and Powell *et al.* (1991).

Perhaps the most important result here is that the equation derived from the mean of the winds from the 600 - 1800 m layer is most successful in predicting the surface sustained wind and gusts with an input wind from any of the levels studied. The average error is 1.4 m/s. Improving the surface wind prediction by selecting a regression equation for a specific level because it had a slightly larger r-squared or smaller mean error is not necessary because of large error variances.

The mean wind direction shift from the surface to 1800 m is a 30 degree clockwise rotation. All but two of the 30 degrees rotation occurs from the surface through 1200 m. An interesting finding in the day and night wind shift data is that the wind shifts from the surface through 1800 m are essentially the same for both the daytime and nighttime data.

Stratification of all of the data into subsets of daytime and nighttime observations reduces the prediction errors of the nighttime winds when the ratio approach is used. Because the daytime prediction errors and variances are larger than those of the nighttime data, only the nighttime predictions are significantly improved.

The wind ratios show that both the surface sustained wind and the surface gusts are higher during the day than the night. For example, the ratio is 0.63 (0.78) for the daytime wind speed (gust) and 0.41 (0.67) for the nighttime wind speed (gust).

The day/night stratifications do improve the mean-layer regression predictions in some cases (relative to the equation from the non-stratified data set). Predictions at low altitudes and with small upper-level wind speeds for both day and

night are significantly improved. However, only daytime gust predictions are improved. Although the results are statistically significant, the actual magnitudes of the speed improvements are less than one m/s over the single mean-layer equation derived from all of the data.

The stratification of all the data into subsets of winds with over-water trajectories ("sea") and those with over-land trajectories ("land") significantly improves the prediction of the "sea" surface winds based on the profiler winds at 600, 1500 and 1800 m. Since 90% of total data set is in the "land" subset, the prediction errors using the ratio approach with the overall data set are not significantly reduced for the "land" winds. Similarly, the mean-layer regression equations for land and sea data do not significantly improve the predictions from the total data set. However, the regression curves demonstrate that the difference between the surface winds over the sea and land is greater as the upper-level winds increase.

The "sea" ratios are larger than the "land" ratios for both the sustained winds and gusts. Although the prediction errors of the sea subset are smaller compared to the total data set, the error reduction is not significant for the gust data. Reduced drag over water allows the surface wind direction and speed to more closely match the upper-level wind. The average wind shift in the first 600 m was found to be 9° for winds over water and 21° for winds over land.

In summary, the accurate prediction of the surface sustained wind and gust is an important problem, especially when associated with tropical cyclones. Although the wind aloft is sometimes known from aircraft observations or low-level cloud-drift wind measurements, the surface wind speed and gust are more often elusive measurements. With the loss of routine aircraft reconnaissance in the western

North Pacific, the problem is exacerbated. In past studies, wind ratios have been used to relate the upper-level winds to the surface winds. Part III of this study demonstrated the usefulness of regression equations for this purpose. Although the equations more accurately predict the surface sustained wind speeds and gusts, the improvements of 1 - 2 m/s over the ratio predictions are not operationally significant.

An alternative use for the ratios and regression equations is to estimate the strength of a tropical storm above the boundary layer at a surface observation reporting site. For example, at 600 m, significantly different ratios are demonstrated at Okinawa for nighttime (0.411) versus for daytime (0.633). If the inverse of these ratios is used to estimate the winds aloft, significantly different tropical cyclone intensities may be inferred.

Although the land/sea comparisons here are suggestive of the expected variations, the surface observations with trajectories over the sea are actually measured about 2 km inland. It would be useful to gimbal a radar wind profiler on a floating platform to obtain true comparisons of the stronger surface winds over the sea and in the vicinity of tropical cyclones.

APPENDIX A: U- AND V-COMPONENT BOX PLOTS
AND 3-D SCATTERPLOTS

Box-plots and 3-D scatter plots similar to those in Figs. 4 and 5 are given here for the u- and v-components within speed and height intervals.

The rawinsonde speed code is as follows: "1" is less than 7.9 m/s, "2" is between 7.9 and 12.5 m/s, "3" is between 12.5 and 19.2 m/s, and "4" is greater than 19.2 m/s.

The height code is as follows: "1" is below 3315 m, "2" is between 3315 and 6010 m, "3" is between 6011 and 7885 m, and "4" is above 7886 m.
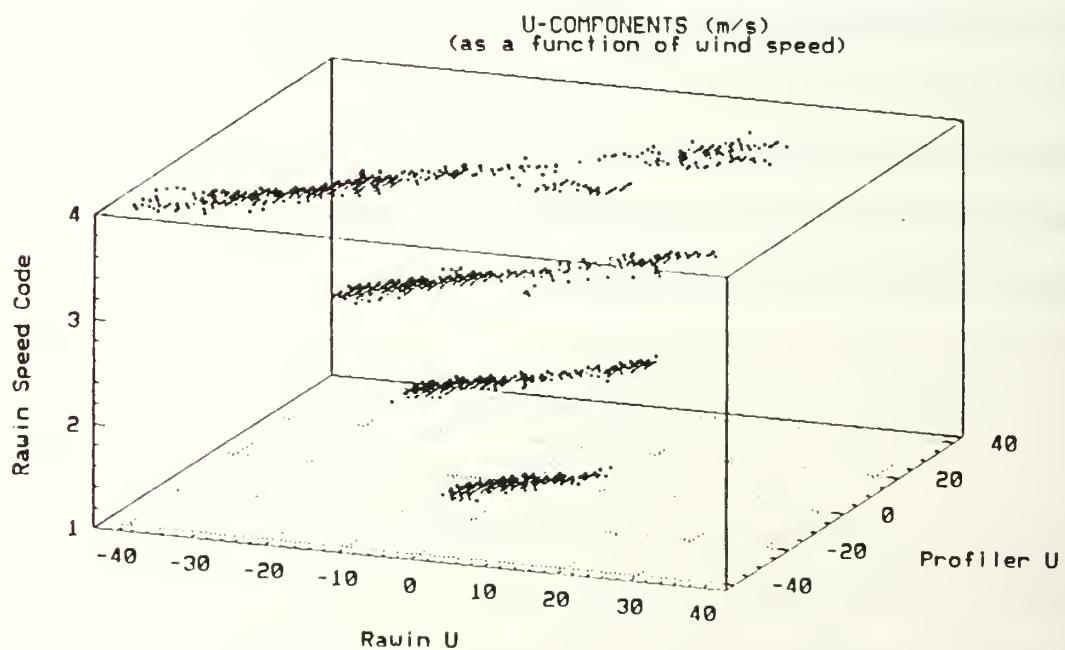

Fig. A-1. Scatterplot for u-components as a function of wind speed.
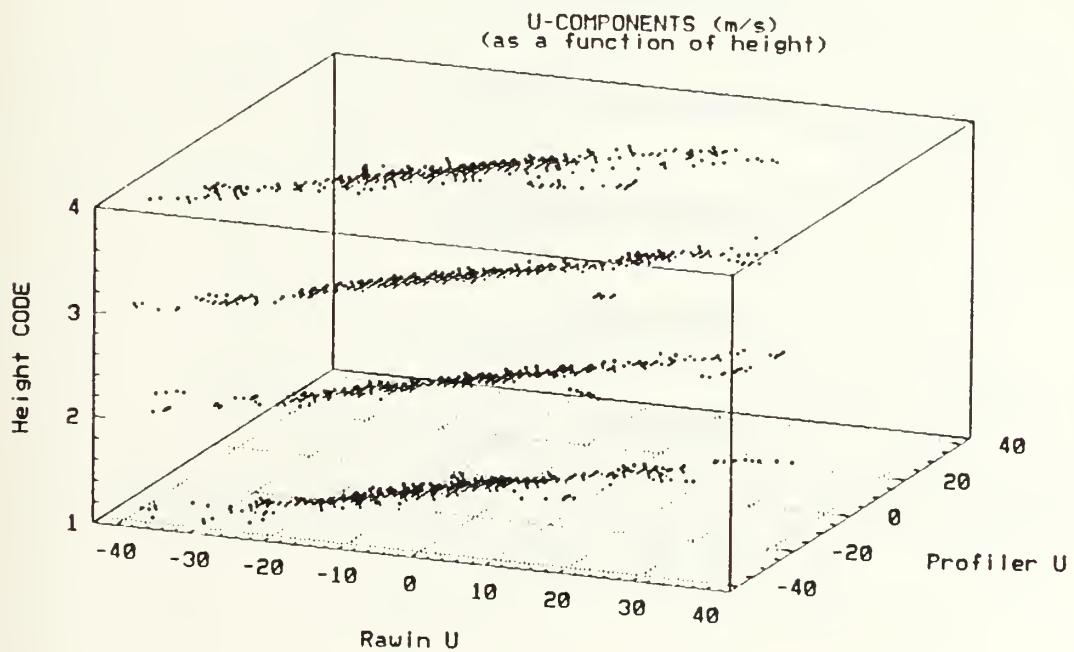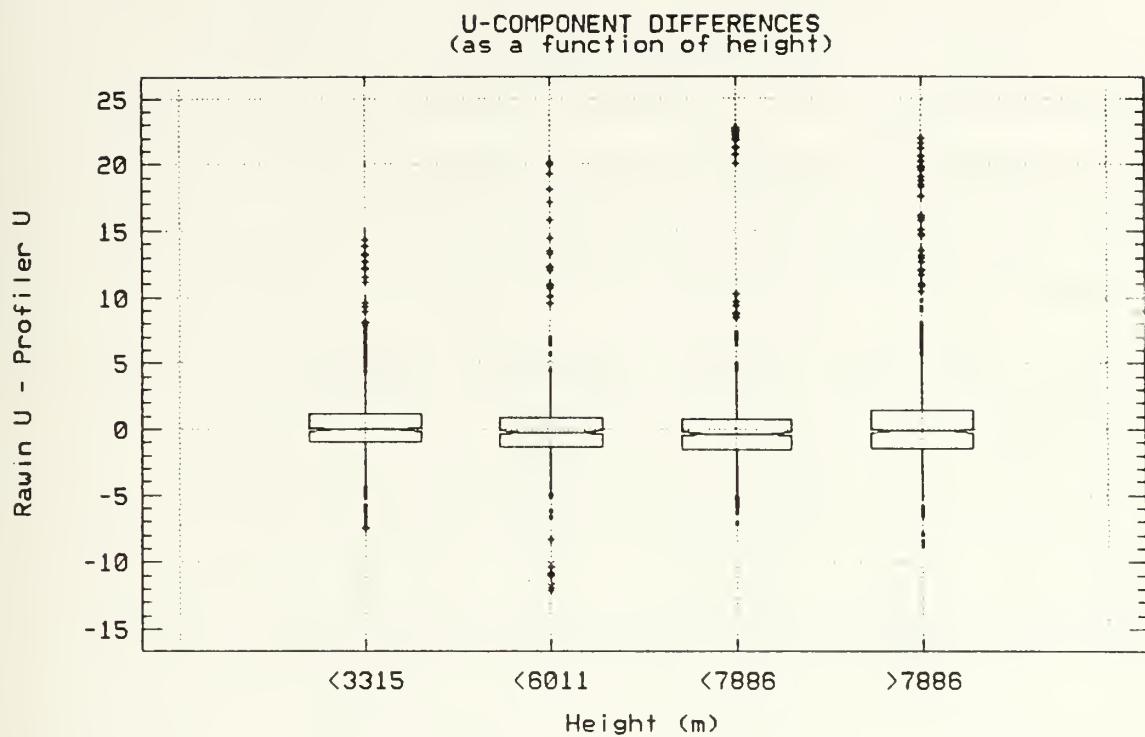
Fig. A-2. Box-plot and scatterplot for u- components as a function of height.
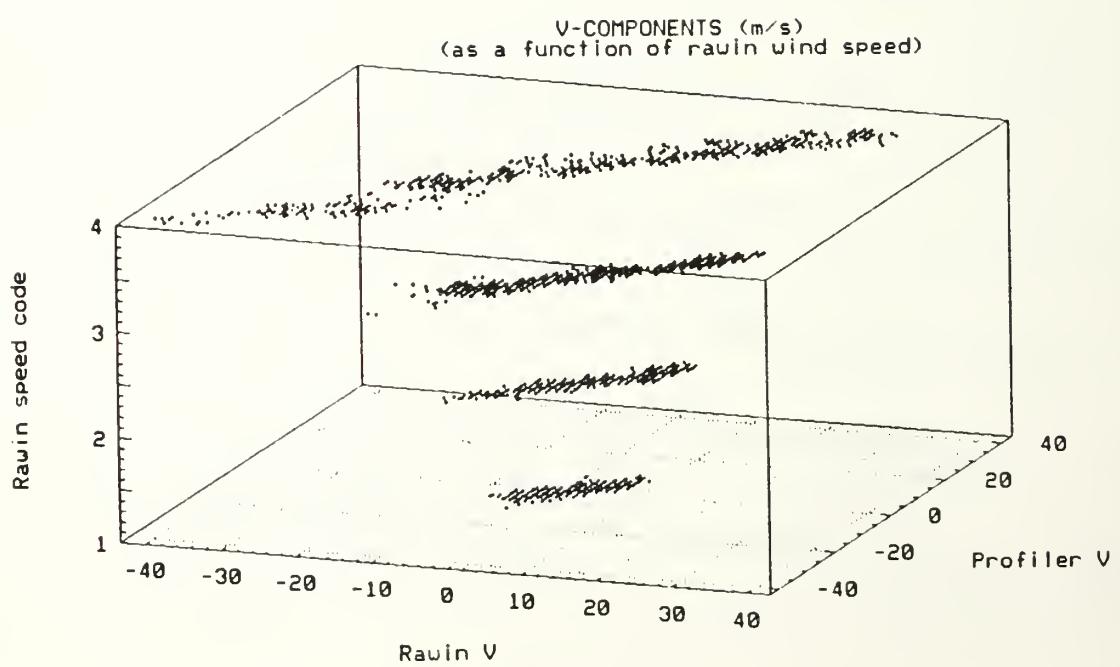
Fig. A-3. Scatterplot for v-components as a function of wind speed.
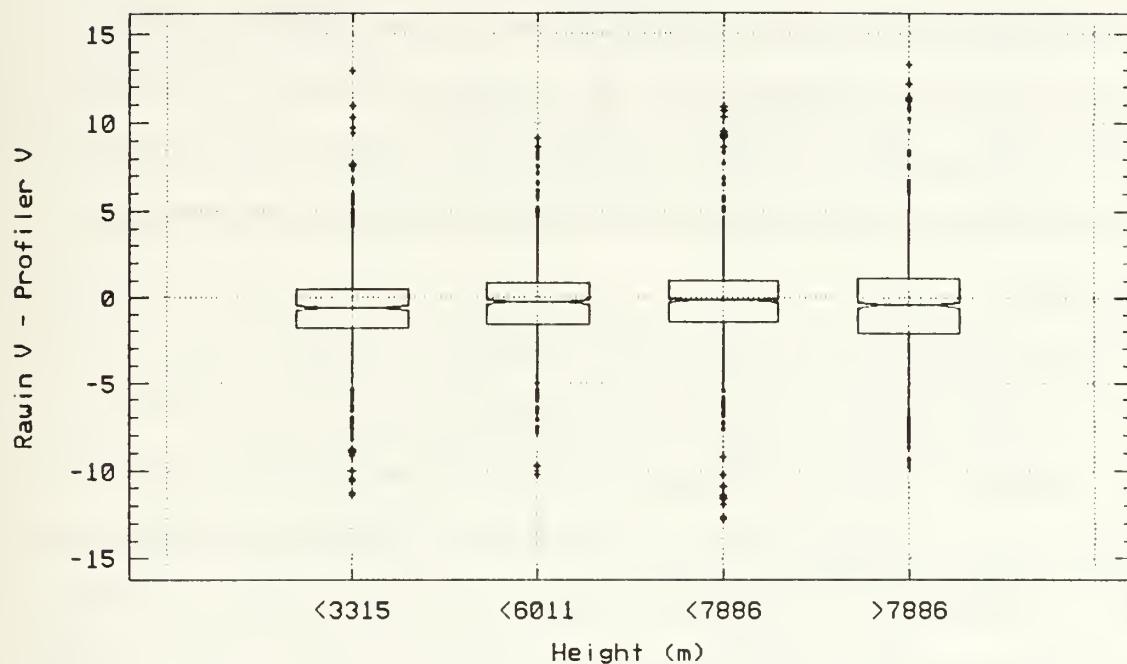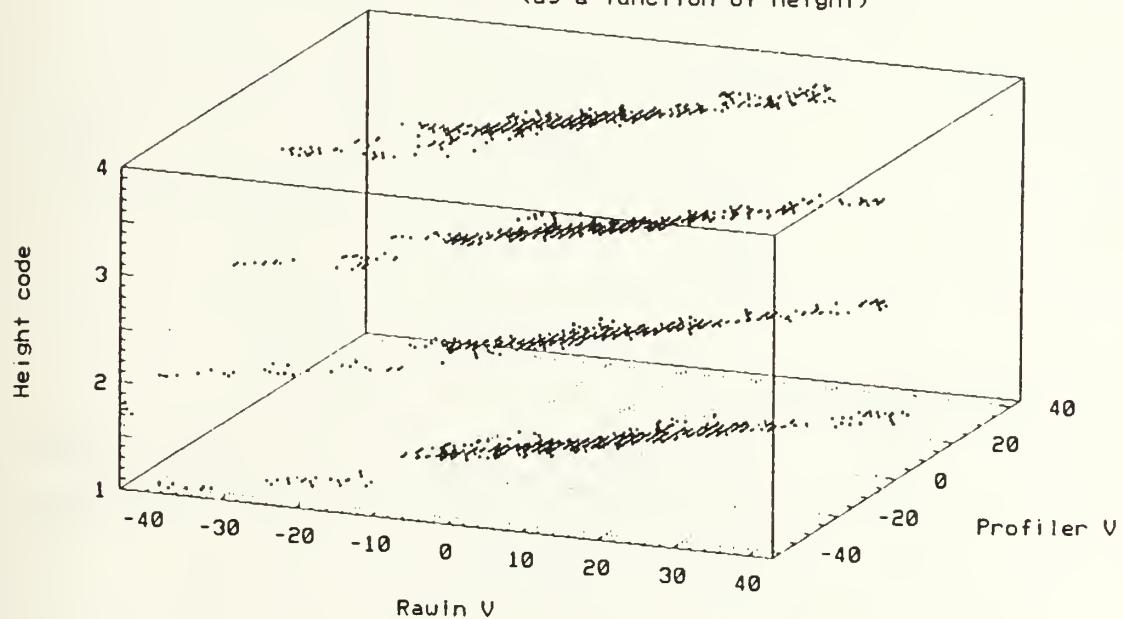
Fig. A-4. Box-plot and scatterplot for v-components as a function of height.

71

APPENDIX B: KOLMOGOROV-SMIRNOV TEST RESULTS

Kolmogorov-Smirnov (K-S) statistics of error distributions are presented. The K-S test is used to determine whether the distribution of prediction errors from two subsets are statistically different. Part 1 has the calculated values for the day and night subsets, while Part 2 shows the K-S values for the land and sea trajectory comparisons.

The left (right) column is for surface sustained wind (gusts). Table entries are used to assess 95% significance levels. If these critical values are equal to or greater than 0.05, then the equation error distributions are not significantly different. Levels 1 through 5 refer to profiler elevations 600, 900, 1200, 1500 and 1800 m. In addition to the comparison of simple ratios between the five levels, the other subsets are separate regressions at each of the five levels, the best equation applied at the five levels, and the mean-layer equation applied at the five levels.

Part 1. Day vs Night

CRITICAL VALUES

	Level	Sustained Winds			Gusts		
		DAY VS ALL	DAY VS NIGHT	NIGHT VS ALL	DAY VS ALL	DAY VS NIGHT	NIGHT VS ALL
RATIOS	1	10^{-4}	0	0	0.67	10^{-3}	10^{-3}
	2	10^{-4}	0	10^{-8}	0.61	0.04	0.04
	3	10^{-5}	0	0	0.02	0.03	0.04
	4	10^{-6}	0	0	0.29	0.06	0.08
	5	10^{-4}	0	10^{-6}	0.25	0.14	0.15
SEPARATE LEVEL EQUATIONS	1	0	0	0	0	0	0.86
	2	10^{-4}	0	0	0	0	0.93
	3	0.04	0	0	0	0	0.94
	4	0.02	0	0.21	0	0	0.95
	5	0.15	0	0.36	0	0	0.52
BEST EQUATION	1	10^{-4}	10^{-3}	10^{-3}	0	0	0.86
	2	10^{-4}	0.06	0.10	0	0	0.89
	3	10^{-4}	0.12	0.14	0	0	0.87
	4	0.02	0.21	0.39	0	0	0.99
	5	0.09	0.36	0.09	0	0	0.76
MEAN-LAYER EQUATION	1	0.02	10^{-5}	10^{-3}	0	0	0.63
	2	10^{-3}	10^{-5}	0.04	0	0	0.96
	3	0.04	10^{-5}	0.14	0	0	0.97
	4	0.04	10^{-3}	0.40	0	0	0.96
	5	0.07	0.04	0.28	0	0	0.80

Part 2. Land vs Sea

CRITICAL VALUES

	Level	Sustained Winds			Gusts		
		LAND VS ALL	LAND VS SEA	SEA VS ALL	LAND VS ALL	LAND VS SEA	SEA VS ALL
RATIOS	1	1.00	0.02	0.02	0.71	0.06	0.09
	2	1.00	0.08	0.10	0.70	0.12	0.22
	3	0.99	0.21	0.32	0.33	0.08	0.25
	4	0.31	10^{-7}	10^{-6}	0.86	0.03	0.02
	5	0.83	10^{-4}	10^{-3}	0.89	0.24	0.21
SEPARATE	1	0.99	0.24	0.25	0.86	0.76	0.95
LEVEL	2	0.99	0.31	0.28	0.95	0.88	0.77
EQUATIONS	3	1.00	0.74	0.68	0.99	0.89	0.97
	4	0.99	0.37	0.20	0.81	0.72	0.84
	5	0.95	0.35	0.29	0.69	0.90	0.98
BEST	1	0.99	0.04	0.06	0.86	0.69	0.41
EQUATION	2	0.99	0.17	0.11	0.94	0.03	10^{-3}
	3	1.00	0.45	0.34	0.85	0.01	0.04
	4	0.99	0.05	0.05	0.96	0.02	0.03
	5	1.00	10^{-3}	10^{-3}	0.67	0.03	0.03
MEAN-LAYER	1	1.00	0.13	0.15	0.95	0.38	0.34
EQUATION	2	1.00	0.26	0.20	0.90	0.95	0.98
	3	0.99	0.60	0.47	0.98	0.97	0.99
	4	0.99	0.43	0.31	0.99	0.54	0.63
	5	0.99	0.07	0.07	0.89	0.69	0.56

REFERENCES

Dobos, P. H., R. J. Lind and R. L. Elsberry, 1991: Doppler radar wind profiler observations from Okinawa during TCM-90. *Preprints of the 19th Conference on Hurricanes and Tropical Meteorology*, Miami, Amer. Meteor. Soc., Boston, MA 02108, 10-15.

Elsberry, R. L., B. C. Diehl, J. C.-L. Chan, P. A. Harr, G. J. Holland, M. Lander, T. Neta and D. Thom, 1990: ONR Tropical Cyclone Motion Research Initiative: Field Experiment Summary. Technical Report NPS-MR-91-001, 107 pp. [Available from the Naval Postgraduate School, Meteorology Department, Monterey, CA 93943.]

Lind, R. J., 1993: Extracting valid winds from rain-contaminated 404 MHz Doppler radar wind profiler data. In preparation for submission to *J. Atmos. Oceanic. Technol.*

May, P. T., 1992: Comparison of wind profiler and radiosonde measurements in the tropics. Unpublished manuscript. Australia Bureau of Meteorology Research Centre, Melbourne.

Ottersten, H., 1969: Radar backscattering from the turbulent clear atmosphere. *Radio Sci.*, **4**, 1251-1255.

Powell, M. D., 1980: Evaluations of diagnostic marine boundary-layer models applied to hurricanes. *Mon. Wea. Rev.*, **108**, 757-766.

----, 1982: The transition of the Hurricane Frederic boundary-layer wind field from the open Gulf of Mexico to landfall. *Mon. Wea. Rev.*, **110**, 1912-1932.

----, P. P. Dodge and M. L. Black, 1991: The landfall of Hurricane Hugo in the Carolinas: surface wind distribution. *Wea. Forecasting*, **6**, 379-399.

Thomson, D. W., and S. R. Williams, 1991: Analysis of comparative wind profiler and radiosonde measurements. *Seventh Symposium on Meteorological Observations and Instrumentation*, New Orleans, Amer. Meteo. Soc., 281-284.

van de Kamp, D. W., 1988: *Principles of Wind Profiler Operation - Training Manual #1*. Office of Meteorology, National Weather Service, 50 pp.

INITIAL DISTRIBUTION LIST

		No. Copies
1.	Defense Technical Information Center Cameron Station Alexandria, VA 22304-6145	2
2.	Library, Code 52 Naval Postgraduate School Monterey, CA 93943-5000	2
3.	Prof. T.R. Holt (Code MR/Ht) Department of Meteorology Naval Postgraduate School Monterey, CA 93943-5000	1
4.	Chairman (Code MR/Hy) Department of Meteorology Naval Postgraduate School Monterey, CA 93943-5000	1
5.	Prof. R.L. Elsberry (Code MR/Es) Department of Meteorology Naval Postgraduate School Monterey, CA 93943-5000	2
6.	Mr. Paul H. Dobos Department of Meteorology Naval Postgraduate School Monterey, CA 93943-5000	1
7.	Director Naval Oceanography Division Naval Observatory 34th and Massachusetts Avenue NW Washington, DC 20390	1
8.	Commander Naval Oceanography Command Stennis Space Center MS 39529-5000	1
9.	Commanding Officer Fleet Numerical Oceanography Center Monterey, CA 93943-5005	1
10.	Director Naval Research Laboratory Monterey, CA 93943-5006	1